A Review of the Thermochemistries of Biomass Gasification and Utilisation of Gas Products

Carine T. Alves[1,2], Jude A. Onwudili[1, *], Payam Ghorbannezhad[3], Shogo Kumagai[4,5]

[1]Energy and Bioproducts Research Institute, School of Infrastructure and Sustainable Engineering, College of Engineering and Physical Sciences, Aston University, Aston Triangle, Birmingham B4 7ET, UK

[2]Energy Engineering Department, Universidade Federal do Reconcavo da Bahia, CETENS, Av. Centenario 697, Feira de Santana, 44.085-132

[3]Department of Biorefinery, Faculty of New Technologies Engineering, Shahid Beheshti University, Tehran, Iran.

[4]Graduate School of Environmental Studies, Tohoku University, 6-6-07 Aoba, Aramaki-aza, Aoba-ku, Sendai, Miyagi 980-8579, Japan

[5]Division for the Establishment of Frontier Sciences of Organization for Advanced Studies, Tohoku University, 2-1-1 Katahira, Aoba-ku, Sendai 980-8577, Japan

Abstract

Conventional biomass gasification involves a complex set of chemical reactions leading to the production of a product gas mainly composed on carbon monoxide, hydrogen, carbon dioxide and methane. Some C_2 -C_{5+} hydrocarbon gases are also formed in the gasifier. This review has uniquely focused on the thermochemistries of conventional biomass gasification with emphasis gasification temperature, gasifying agents (pure oxygen, air, carbon dioxide, steam or combinations of these) and the types of gasifiers as the key parameters that determine the yields and compositions of gas products. With air as gasifying agent, the product gas is highly diluted with nitrogen (> 45 vol%) and is known as producer gas, which is often more suitable for direct energy application via combustion. With nitrogen-free gasifying agents, syngas with ≤ 5 vol% nitrogen content is produced, and therefore suitable for various downstream uses including enhanced hydrogen production via water-gas shift reaction and, especially, synthesis of organic compounds such as methanol and dimethyl ether as well as hydrocarbons (liquids and waxes via Fisher-Tropsch synthesis). The contributions of kinetic and thermodynamic studies to the understanding and progress of biomass gasification have been explored. In addition, the review covers the challenges of tar formation during biomass gasification and various strategies to reduce/eliminate this major bottleneck via catalysis and reactor design or configuration. The historical perspective of biomass gasification and current trends are presented, highlighting the exponential growth in high-quality research publications around biomass gasification over the last decade, possibly driven by current Net Zero initiatives.

Keywords: biomass gasification, thermochemistries, kinetic and thermodynamic modelling, renewable fuel gas, renewable hydrocarbons, Net Zero

* Corresponding author (j.onwudili@aston.ac.uk)

1.   Introduction

Plants transform energy from the sun into chemical energy, which is stored as renewable organic materials known as biomass through the process of photosynthesis. Apart from animal manure and human wastes (sewage), all types of biomass feedstocks used for energy are directly derived from plant matter. With growing experience in biomass chemical energy utilisation, there is a realization that the most sustainable biomass feedstocks are those that hardly complete with food production and are known to have positive impacts on land use [1]. This recognition of sustainable biomass's contribution to global low-carbon energy development and achievement of Net Zero has been the main driver of the consistent growth witnessed in the last three decades around bioenergy technologies. For instance, the bioenergy sector grew at an annual rate of 2% between 2000 and 2018 [2]. By 2019, global capacity of wood fuel was estimated to be about 1.9 billion m^3 from which nearly 40 million tonnes of wood pellets were produced for bioenergy applications [2]. From Figure 1, the most abundant biomass feedstocks are based on lignocellulosic biomass comprising of wood and wood processing wastes as well as agricultural wastes [3]. There are therefore increasing expectations for sustainable biomass to contribute to the reduction of emissions of greenhouse gases, particularly carbon dioxide. One way of achieving this is to deploy point-source CO_2 capture during large-scale bioenergy production, which can lead to negative emissions and therefore reduce the impact of climate change and global warming.
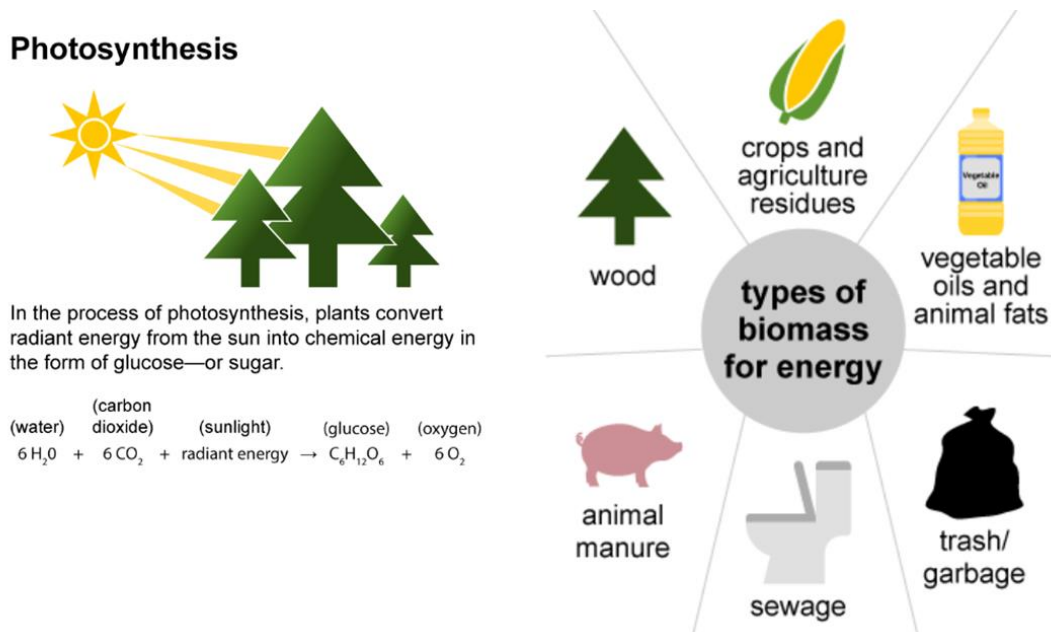

Figure 1: Sources of biomass for energy production (Source: Biomass explained - U.S. Energy Information Administration (EIA)) [3]

In general, biomass has the potential to produce energy vectors than can satisfy significant proportions of the global primary energy demand sectors – heating (industrial, residential and commercial), electricity and transport [3]. Lignocellulosic biomass provides the options to obtain different energy products via a range of conversion technologies, including chemical, thermochemical and biological processing routes.

Among the thermochemical technologies (Figure 2), direct combustion is the main route widely used to convert biomass for heat and power generation. Industrial-scale combustion involves burning biomass feedstocks in plentiful of oxygen in a highly exothermic reaction and the heat recovered for use in steam-cycles and/or gas turbines for electricity generation. In combined heat and power systems, residual heat after electricity generation is further used for heating purposes. With the advent and growth of heat pumps and other low-heat recovery systems, there are chances to improve energy efficiencies of CHP plants based on biomass combustion.

Pyrolysis occurs in the absence of air or oxygen/oxidant to transform biomass into a mixture of liquid, solid and gaseous energy vector products at temperatures ranging from 400 – 600 °C. The pyrolysis process can be tuned to favour any of the three products as the main product depending on a number of factors including heating rate, vapour residence times, reactor types, temperature and type of biomass [4]. Pyrolysis is an endothermic process, requiring energy input to promote the breaking of covalent bonds in the molecular structure of biomass.
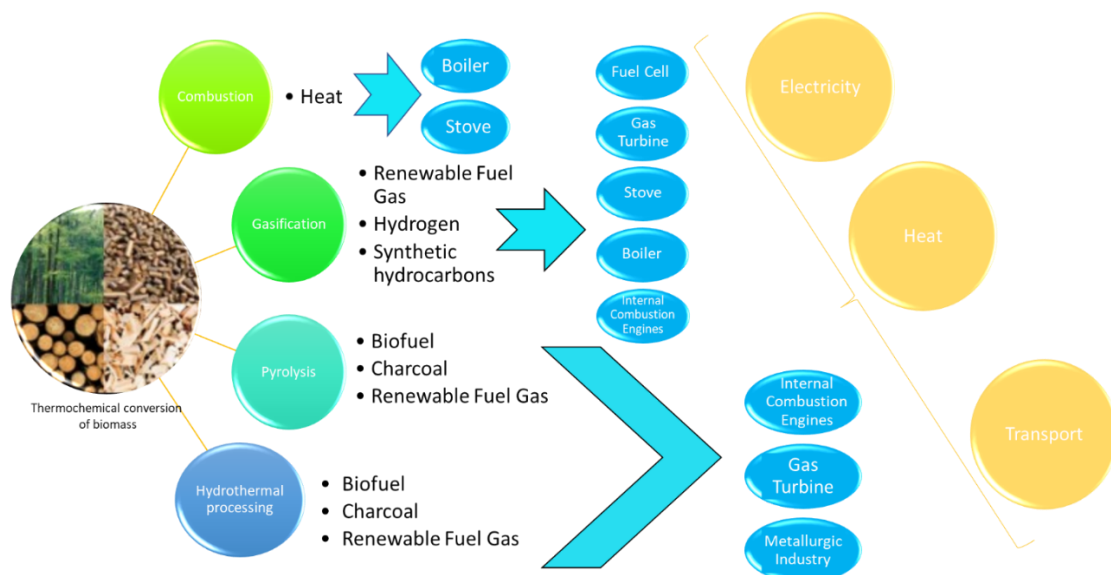

Figure 2: Thermochemical routes for biomass conversion, indicating the versatility of energy products

Gasification is another thermochemical technology that converts solid carbonaceous fuels to gas products for subsequent applications. The conventional gasification process involves heating organic materials to between 800 °C and 1000 °C, in the presence of controlled and limited amounts of oxidant (gasifying agents), mainly oxygen, air, carbon dioxide or steam. In all cases, the gasification process targets the conversion of solid biomass into a gas product with high concentrations of carbon monoxide and hydrogen, which can be used directly or indirectly for energy applications as well as chemical production.

There are clear indications that the future of combustible energy belongs to low-carbon fuel gases, including hydrogen, ammonia, dimethyl ether (DME) and hydrocarbon fuel gases such as methane propane and butane [5]. Among these gases, hydrogen, hydrocarbon fuel gases and DME can be commercially obtained from the conversion of solid biomass feedstocks via gasification technology,

followed by suitable chemistries [6]. This present review has focused on the extensive thermochemistries involved in the biomass gasification process, with emphasis on how the reaction conditions influence the various reactions and therefore, influence the biomass gasification efficiency as well as yields and compositions of the gas products. In addition, the thermodynamic and kinetic analyses of biomass gasification are discussed in relation to how these have helped to improve the understanding and efficiency of biomass gasification technology for scaling up to commercial reality. Further, sections are dedicated to the influence of catalysts during biomass gasification and the various catalytic requirements relating to tar reduction, the promotion of the selectivities of certain favourable reactions and also the mechanisms of catalyst deactivation. In addition, the chemistries involved in the utilisation of the gas products obtained from biomass gasification have been reviewed.

2. Historical aspects of gasification

Gasification technology has been in use in one variant or another to convert solid fuels (coal and biomass) to two main gas products (syngas or producer gas) for over 200 years [7]. The application of gasification for biomass conversion was initially developed in the 1800s to produce town gas for lighting and cooking. During the 1920s, its use was extended to blast furnaces and synthetic fuel production and by the World War II, biomass gasification was used to produce transportation fuels through the well-known Fischer-Tropsch (FT) synthesis [8]. In modern times, the many advantages of this technology are being exploited for bioenergy production and utilisation in domestic heating and cooking, synthetic liquid biofuels and chemical production, power generation and renewable biohydrogen production.

Broadly speaking, the gas products are often differentiated by the gasifying reagent that is reacted with the solid feedstock. Syngas is produced when pure oxygen, steam or a mixture of both is used as gasifying agent, while producer gas come from when the solid fuel is reacted with air. Hence, syngas and producer gas can be differentiated by their nitrogen contents are shown in Table 1. The use of gasification to convert solid biomass to gas products with mostly well-defined compositions, provides of routes for a variety of applications.

Table 1: Typical compositions of producer gas and syngas differentiated by the nitrogen contents resulting from the use of different gasifying agents [7].

Component	Producer gas	Syngas
Carbon monoxide (vol%)	18 - 22	35 - 40
Hydrogen (vol%)	13 - 19	20 - 40
Methane (vol%)	1 - 5	0 - 15
Carbon dioxide (vol%)	9 - 12	25 - 35
Tar (vol%)	0.2 - 0.4	-
Nitrogen (vol%)	45 - 55	2 - 5
Moisture (vol%)	4.0	Variable
Lower Heating Value (LHV), MJ/Nm^3	4.5 – 6.0	5.3 - 12.6

2.1. Modern trends in biomass gasification research

The last two decades have seen an exponential growth in biomass gasification research, leading to commercialisation of the technology at different scales. Between 1999 and 2023, a total of 8,698 articles (keywords: "Biomass gasification"; "sources" OR "source"; "energy" AND "analysis") were published on the ScienceDirect website in the field of biomass gasification. These included about 85.5% experimental research articles and 14.5% reviews. According to Figure 3, in the last 14 years this area has notoriously grown internationally in terms of volume of high-quality articles published with increasingly consolidated research groups. In terms of journals, the International Journal of Hydrogen Energy and Energy have published the majority of articles in this area, corresponding to 20% of the total number of articles published.
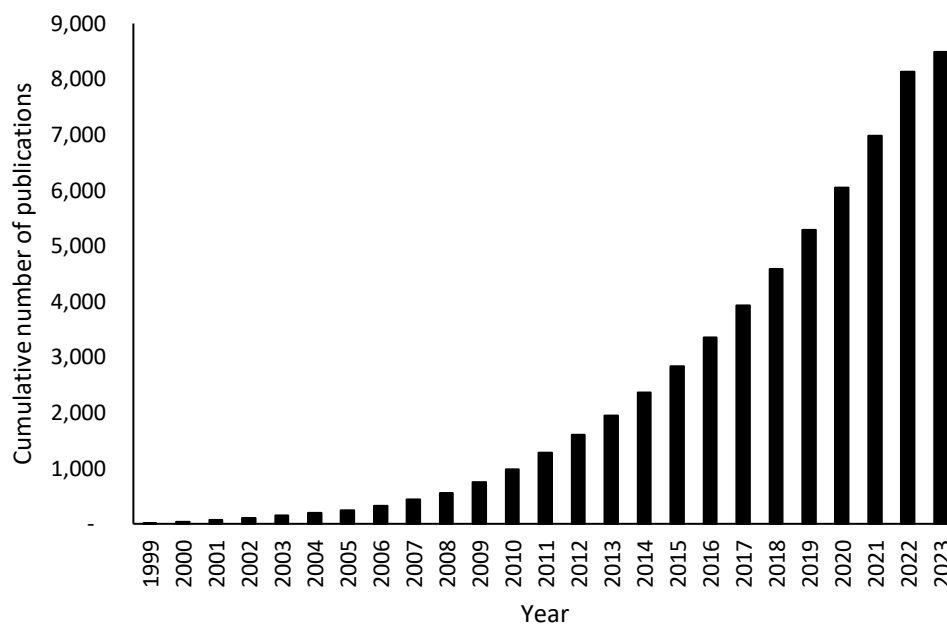

Figure 3: Papers published between 1999-2023 (ScienceDirect website)

Several reviews have been published recently about biomass gasification [9-15]. These reviews covered various aspects of the technology, including the effects of gasifier designs, temperature, pressure, steam-to-biomass (S/B) ratio, steam flow rate, moisture and biomass particle sizes and catalysts on biomass conversion and gas products yields. For example, Hoang, et al., [10] recently publised a review on the key factors that affect the hydrogen yield from steam gasification of lignocellulosic biomass. In addition, Mishra and Upadhyay [11] critically reviewed the past and present status of the overall biomass gasification research, including technologies and parameters involved in the production of syngas, biofuels, biochar, power, heat and fertilizers. Furthermore, Safarian, Unnþórsson and Richter [12] reviewed biomass gasification modelling to generate and analyze statistics on the growing number of studies and approaches used in this field.

3. Biomass gasification process

Biomass gasification is a thermochemical process that usually occurs between 800 °C - 1000 °C producing carbon monoxide (CO), hydrogen (H_2) and methane (CH_4) as main products. Carbon dioxide (CO_2) and other hydrocarbons (HC) are also obtained as co-products. Nitrogen (N_2) is also present in the gas product but can come from the gasifying agent and the biomass feedstock [13 – 15]. The yield and quality of the gas product depends on several factors, including mainly the biomass type and particle size, the gasifying agent, the type of gasifier (reactor), the ratio of biomass to gasifying agent and other operating conditions of the process. The main equation for the gasification process may be represented as Equation 1:

$$CH_X O_Y N_Z + wH_2 O + m(O_2 + 3.76N_2) \rightarrow n_1 H_2 + n_2 CO + n_3 H_2 O + n_4 CO_2 + n_5 CH_4 + n_6 N_2 \quad (1)$$
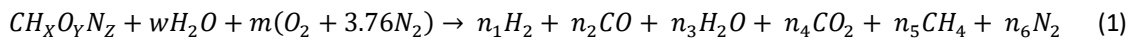
where n_1 to n_6 are the stoichiometric coefficients; $CH_X O_Y N_Z$ is the biomass formula, w is the molar amount of moisture in the biomass.

The main chemistry of biomass gasification can be described as a limited oxidation process that involves various stages of solid conversion to gas, with simultaneous formation of little amounts of solid residue (char and ash) and condensable compounds (tar) [10 -12]. Biomass gasification efficiencies are often higher than 50% [11], which makes the technology highly promising for low-carbon future energy vectors, particularly hydrogen.

Figure 4 shows the classical biomass gasification process, comprising of the three main processing steps: biomass preprocessing, the gasification technology and downstream processing. The methods of gas product utilisation is an addition downstream step and comprises may potential possibilities for green energy, fuels and chemicals.

Physical processes	Chemical and physical processes	Physical and chemical processes	Chemical and mechanical processes
Harvesting	Heating	Tar removal	Gas turbine - power
Drying	Various chemical reactions	Particulate removal	Gas burner – combined heat & power
Transporting,	Gas production	Steam reforming	Fuel cells
Size reduction e.g.,		Water-gas shift	Methanol synthesis
cutting, milling,		CO_2 capture	Dimethyl ether (DME) synthesis
Densification e.g.,		Excess water removal	Hydrocarbon synthesis (FT)
pelletisation,			
torrefaction, etc.			

Biomass pre-processing	Biomass gasification (800 – 900 °C)	Gas product clean-up and conditioning	Utilisation of gas product

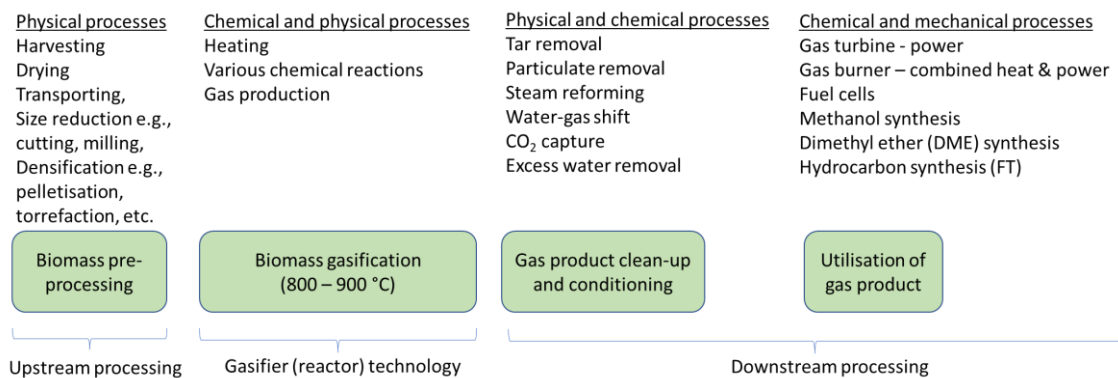| Upstream processing	Gasifier (reactor) technology	Downstream processing

Figure 4: Classic biomass gasification process

As shown in Figure 4, solid biomass feedstocks such as wood and agricultural residues need to be pre-processed (mostly into pellets) before feeding into the gasifier for several reasons. For instance, freshly harvested lignocellulosic biomass naturally has high moisture and is also highly fibrous due to the presence of non-crystalline components such as lignin and hemicellulose. These properties make milling

difficult. Drying, size reduction through cutting, milling and eventual pelletisation are pre-processing steps often carried out to deliver the feedstock in the right particle size, moisture contents (usually < 10 wt%) for gasification reactions. Drying can be achieved by using waste heat from the gasification process, and the process of drying is often accomplished using perforated bin dryers [13], band conveyors [14] and rotary cascade dryers [15]. Pre-processing of biomass up to pellet production consumes between 100 – 200 kWh per tonne, which can be between 2 – 3 % of its energy content [16].

Torrefaction, which involves the mild heating of biomass at temperatures of around 280 °C and atmospheric pressures, has also become an important biomass pre-treatment step to reduce moisture contents and improve the grindability of biomass. The torrefaction process can reduce the amount of mechanical energy expended during biomass milling and has also been found useful for pelletisation. Making biomass pellets is also important to reduce transportation costs. Wood chips naturally has low density of around 300 kg/m^3, so that pelletisation process can both reduce the moisture contents as well as increase the density to up to 600 – 800 kg/m^3 [16].

On delivery to gasification plants, the biomass pellets are usually however milled to finer particle sizes using hammer mills, knife mills, small-capacity tub grinders and screens to achieve the desired particles sizes of usually between 150 μm– 600 μm [17]. This range of particle size facilitates efficient heat transfer, which promotes fast gasification rates due to rapid and uniform heating with insignificant particle temperature gradient [18]. Particle below 150 μm may be blown out of the gasifier before they even react while heaver particles above 600 μm may be too slow to gasify and thus also leave the gasifier without complete conversion [19]. In addition, literature has shown that smaller particle sizes can result in the formation of more methane, CO and other hydrocarbon gases, while reducing CO_2 formation [19].

3.1. Biomass gasifiers and their main features

Biomass gasification can be accomplished in several types of gasifiers, broadly classified as fixed beds and fluidised beds. Between the fixed bed gasifiers and the fluidised beds, the main difference is that fixed beds have well-defined reaction zones, whereas fluidised beds do not. In fluidised bed gasifiers, silica or alumina, which have high specific heat capacities and thermal stability are used as bed materials [20]. In some cases, catalysts may be added with the bed material [21]. The gasifying agent fluidises the bed and the biomass, leading to enhanced heat transfer, increased reaction rates, short residence times and higher conversion efficiencies compared to fixed bed gasifiers [22]. Some relatively new and innovative gasifiers such as the entrained flow gasifiers [23] and plasma gasifiers [24] and fountain enhanced spouted conical gasifiers [28] appear to be promising in terms of gasification efficiencies as shown in Tables 2a - 2c [23 – 28],

Fluidized bed gasifiers, including bubbling and circulating fluidized bed reactors, have gained popularity in biomass gasification research and industrial applications [25 – 27]. These gasifiers provide several

advantages, including efficient mixing of biomass with the gasifying agent, high throughput processing, uniform temperature distribution throughout the reactor, and enhanced heat transfer between the solid biomass particles and the gas phase. These features contribute to improved gasification kinetics by promoting rapid reactions and maximizing the utilization of biomass feedstock. The advanced control of temperature and residence time in fluidized bed gasifiers allows for better optimization of gasification conditions, leading to higher syngas yields and improved overall process efficiency.

In fixed bed gasifiers, distinct reaction zones can be identified unlike in fluidized beds (Table 2a). The main differences among the fixed bed gasifiers are the directions of flow of biomass and gasifying agents. Downdraft gasifiers operate in a co-current manner, with biomass and the gasifying agent introduced from the top. The co-current flow pattern ensures that the desired gasification reactions occur in the optimal temperature range, enabling higher conversion of the biomass into syngas, promoting efficient tar cracking, leading to cleaner syngas production [23 – 25]. For updraft fixed bed gasifiers (biomass flows from top and gasifying agent from bottom), like the downdraft type, well-defined zones for biomass drying, pyrolysis, reduction and combustion can be observed [25 – 27]. Hence, as main feature, updraft gasifiers have high thermal efficiency due to the positioning of the combustion zone at the bottom bed, while hot gases sequentially pass through the reduction, pyrolysis and drying zones. The main disadvantage of the updraft fixed bed gasifier is the excessive formation of a complex and often corrosive mixture of condensable vapours known as tar. Biomass throughputs are generally lower when using fixed gasifiers and startup times are longer than in fluidised beds. A major advantage of crossflow gasifiers is that they have faster startup times compared to downdraft and updraft gasifiers.

Table 2a: Typical features of fixed bed biomass gasifiers [25-27]
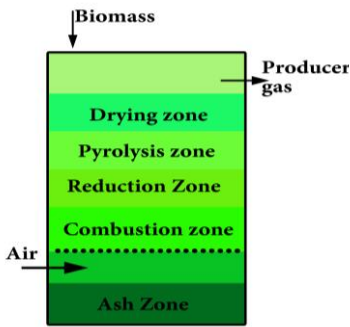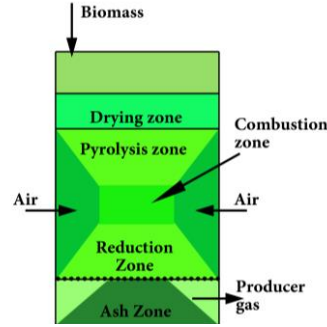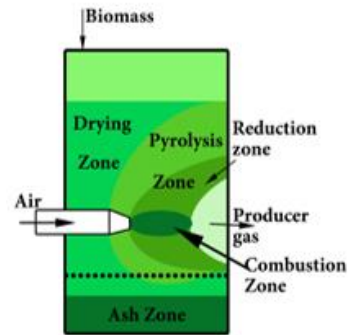
Updraft	Downdraft	Cross draft
• Counter current flow of biomass (downwards) and gasifying agent (upwards). • Ash is removed at the bottom as dry ash or slag (if temperature is high enough to melt ash compounds). • Well-defined zones for combustion zone (1090 °C) at the bottom, a gasification (reduction) zone in the middle, and pyrolysis and drying zones at the top. High thermal efficiency but low biomass throughput. • Produces excessive tar yields (up to 50 g/Nm^3). • Biomass particle size >51 mm. • Cold gas efficiency around 80%. • Exit product gas temperatures of 450 °C - 650 °C. • Throughputs of between 200 and 5000 KW$_{th}$.	• Co-current flow of biomass and gasifying agent (usually both downwards). • Well-defined zones for combustion zone (1100 °C) at the middle, a gasification (reduction) zone at the bottom, and a pyrolysis and drying zones at the top. • Much lower tar levels compared to Updraft (<1 g/Nm^3). • Requires tighter specifications on the fuel; 1-30 mm size, low ash, moisture <30%. • Slagging or sintering of the ash in the combustion zone can be an issue. • Similar cold-gas efficiency and range of throughputs as Updraft. • Lower overall efficiencies compared to Updraft. • Exit product gas temperature of around 800 °C. • Overall preferred to Updraft for direct product gas use in internal combustion engines. • Throughputs usually small like those of Updraft.	• Biomass is fed from the top and air enters sideward to create a crossflow arrangement. • The combustion zone is smaller than Updraft and Downdraft, but the reduction and pyrolysis zones extend above and below the combustion zone. • Operating and gas exit temperatures are high. • Can work at high gas velocities and high load capacities (up to 8000 KW$_{th}$), but CO_2 reduction is poor. • Faster start-up time than even Downdraft. • Improved efficiencies with dry fuel.

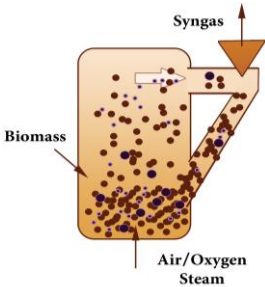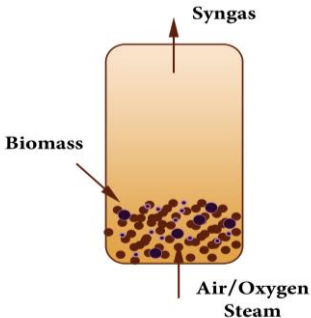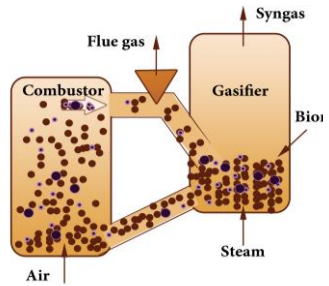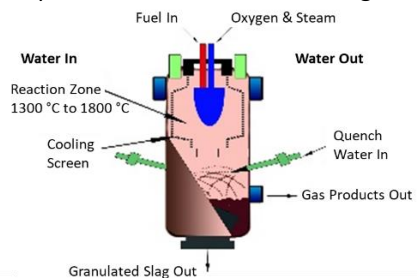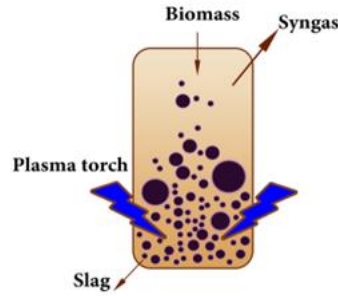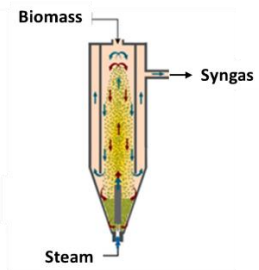Table 2b: Typical features of fluidised bed biomass gasifiers [25-27]

Circulating fluidised beds (CFB)	Bubbling fluidised beds (BFB)	Dual fluidised beds (DFB)
• Biomass is fed from the bottom and fluidizing agents move biomass and bed materials. • Gas stream passes vertically up through a bed of inert particles, resulting in a turbulent gas-solid mixture. • Fuel makes up only a small fraction of the solid. • Can easily be scaled to large capacities. • No segregation of combustion, pyrolysis and reduction zones, simultaneous gasification at all locations. • Uniform bed temperature (around 900 °C) and concentration. • Bed promotes tar cracking and gas-phase cracking in freeboard. • Fluidisation enhances heat transfer, increases reaction rates and conversion efficiencies with tar yields typically between 5 – 10 g/Nm^3. • High throughputs of up to 80000 KW$_{th}$; for large-scale plants. • Tolerates wide variations in biomass types and characteristics and particle sizes of around 6 mm. • Ash and bed materials are separated from the gas product using e.g., cyclone and recirculated. • Typically operated at atmospheric pressure but higher pressures possible. 	• Like CFBs in terms of particle sizes, turbulent mixture of solid and gas, absence of segregation of combustion, pyrolysis, and reduction zones. • Fluidisation agent velocity is lower than in CFBs to avoid bed material carry-over beyond the freeboard. • Similar operating temperature as CFB (900 °C) to avoid ash melting and slagging. • Throughputs are lower than those of CFBs; usually 10000 KW$_{th}$. • Can operate at higher pressures. • Tar yields are typically lower than in CFBs; between 1- 5 g/Nm^3. 	• Similar features of CFB and BFB combined. • Comprises of separate CFB and BFB reactors. • Mostly, steam is used as gasifying agent to convert biomass to nitrogen-free syngas and char in the BFB. • Char is combusted in the CFB using air to heat up the bed. • The hot bed material is fed back into the BFB for steam gasification. • Operated at around 900 °C to avoid ash melting. • Can also be operated at higher pressures.

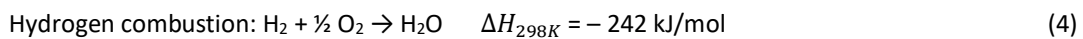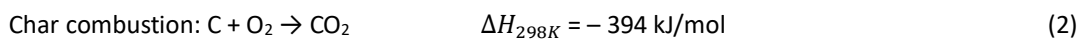Table 2c: Typical features of novel biomass gasifiers [23, 24, 28]

Entrained flow gasifiers	Plasma gasifiers	Fountain enhanced spouted conical gasifiers
• Only dry pulverised biomass can be used. • The high oxygen requirement is used as the gasifying agent into which the biomass particles are entrained. • Biomass combusted with oxygen in a dense cloud of fine biomass particles at the top of a vertically installed cylindrical vessel. • Syngas exits at the bottom of the gasifier and passed through gas cleaning equipment (e.g., cyclone). • Operates at high temperatures (1000 °C- 1900 °C) and high pressures (30 - 70 bar), with exit gas temperature > 1260 °C. • Virtually no tar nor methane is found in the gas products. • Lower thermal efficiencies than other gasifier types and due to high operating temperatures, gas products must be cooled before cleaning. • Particle size used <0.15 mm, so good tolerance to fines but poor to coarse materials. • Milling energy is a considerable cost. • High temperatures convert ash into slag.	• Typically used for unsorted municipal solid waste, biomedical waste and other hazardous wastes. • Whole, untreated biomass can be gasified directly if they can be fed into the gasification chamber. • Converts organic matter into high quality syngas and inorganic matter vitrified into slag. • Process uses an electrically generated plasma torch formed from strong electric current under high voltage. • Temperature around the torch can reach between 1500 °C and 13900 °C, depending on metal used (copper, tungsten, hafnium or zirconium) in the presence of argon (inert gas) • High temperatures and oxygen-lean. atmospheres prevent formation of toxic. compounds (dioxins/furans, NOx and SOx). • Gasification rates of >99% achievable. • Gas cleaning possible with additional plasma arc.	• A recent invention incorporating a novel fountain confiner with the advantages of conventional spouted conical reactors. • Similar gasification conditions as conventional fluidised beds (e.g., 850 °C). • Fountain confiner system increases vapour residence times and avoids entrainments of bed materials and subsequent elutriation. • Provides flexible and highly stable hydrodynamics, so can handle fine catalyst and bed materials. • Characterised by extended flow path for volatiles, which narrows the residence time distribution. • Highly improved contact between volatiles and bed/catalyst material leading to enhanced gasification efficiency. • Potential for significant tar reduction (around 5 g/Nm^3) compared to conventional fluidized beds.

3.2. Biomass gasification chemistries

Biomass gasification involves a series of chemical reactions that combine to yield either syngas or producer gas as the main product (Table 1). Apart from the main components of the gas products, other vapour phase products such as undesirable gases like hydrogen sulfide (H_2S), hydrogen chloride (HCl) and COS (carbonyl sulfide) as well as heavier hydrocarbons and tars are also present in the exiting hot gas stream [28]. The acid gases can cause corrosion of gasifiers and downstream processing equipment. The tar compounds can condense outside the gasifiers at temperatures between 250 °C and 300 °C. In addition to the gas-vapour products, significant amount of char (solid residue) is also formed. Char is a heterogeneous mixture of ash, unreacted biomass and incompletely converted biomass (mainly carbon). The amount of carbon present in the char depends on the gasification technology and operating conditions, especially the oxidant to biomass ratio and gasification temperature [29]. Char yields are typically within 0.5 wt% and 2 wt% of the biomass (dry-ash-free basis) and can have calorific values of between 25 and 30 MJ/kg [29]. In fixed bed gasifiers, the bed material is the biomass feedstock and the ash present in the char comes from the original inorganic compounds (bound and unbound) present in the biomass. Therefore, in such reactors, the amount of ash recovered from the gas product often depends on the types and compositions of the biomass feedstock [30]. For fluidised beds, the ash may include bed materials that are sufficiently light (e.g., via attrition) to become entrained in the high-velocity gas exiting the gasifier.

In general, biomass gasification is an endothermic process, requiring thermal energy input to break strong covalent bonds that make up the chemical structure. Different arrangements for the supply of the thermal energy requirement have been used. In most cases, the energy required is provided by combusting part of the biomass (allothermal gasification) or through partial oxidation (autothermal gasification) of the biomass in the presence of the gasifying agent (usually oxygen or air). Autothermal gasification is considered to include combustion and endothermic drying, pyrolysis and reduction stages in fixed bed gasifiers [31]. Steam-based biomass gasification requires heat input from sources external to the main gasifier chamber.

The main oxidation processes provide the thermal energy required to start the gasification reactions and to maintain temperatures. Usually, the oxygen requirements are in the order of $1/5^{th}$ to $1/3^{rd}$ of the stoichiometric requirement to combust part pf the carbon and hydrogen in the biomass [16], according to the following Equations 2-4:

Char combustion: $C + O_2 \rightarrow CO_2$ $\qquad \Delta H_{298K} = -394$ kJ/mol $\qquad\qquad$ (2)

Partial oxidation of char: $C + \frac{1}{2} O_2 \rightarrow CO$ $\quad \Delta H_{298K} = -111$ kJ/mol $\qquad\qquad$ (3)

Hydrogen combustion: $H_2 + \frac{1}{2} O_2 \rightarrow H_2O$ $\quad \Delta H_{298K} = -242$ kJ/mol $\qquad\qquad$ (4)

Therefore, the products of combustion are CO, CO_2 and H_2O, and their concentrations in the exit gas from the gasifier can give an indication of the dominant reaction stage. Significant amounts of nitrogen will also

be present in the gas products if air has been used as oxidant. As the gas gets hotter, it provides thermal energy for biomass drying within the gasifier. Drying is endothermic and often considered complete when the biomass temperature reaches around 120 °C - 150 °C [32]. The water vapour being expelled during the drying process may participate in further gasification reactions. Therefore, the main hydrogen producing step during non-steam gasification often includes the reaction of the water vapour removed during in-situ biomass drying.
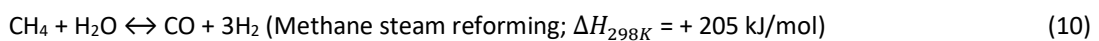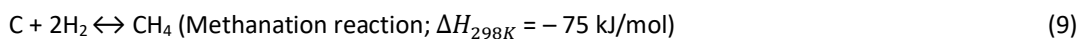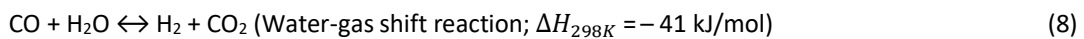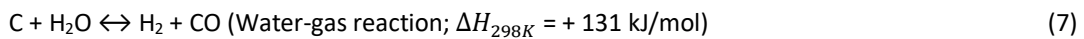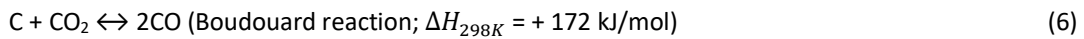
After drying, the endothermic pyrolysis stage sets in, taking place between a wide range of temperatures from 250 °C – 700 °C. It is during the pyrolysis stage that most solid and volatile products are formed.

The pyrolysis stage can be represented by Equation 5.

Biomass → H_2 + CO + CO_2 + CH_4 + H_2O + C_nH_m + tar + solid (overall ΔH is positive) (5)

Fixed bed reactors produce 20 – 25% solids compared to 5 – 10% from fluidised beds [33 - 34]. In general, the solid products from fixed bed reactors contain higher carbon contents mixed with inert solid materials from the biomass ash [33]. Essentially, the solid residues from fixed bed gasifiers have higher heating values than those from fluidised beds [34]. Ideally, the pyrolysis process may produce light organic compounds such as hydrocarbon gases and other organic vapours. However, these organic volatiles (70 – 90 %) are difficult to isolate due to their consumption in the next stage of gas-forming reactions. Hence, only tar products are considered as the surviving liquid products from the pyrolysis stage. The formation of tars varies with the type of gasifier used [25 – 28]. Downdraft fixed bed gasifiers produce low tar yields in the range of 1%, while updraft fixed bed gasifiers can produce between 10 -20 % tars [16]. For fluidised bed gasifiers, tar yields range from about 1 – 5% [25 - 28]. Minor components such as acid gases (H_2S and HCl) may be produced during the pyrolysis stage [35].

Equilibria-based reduction reactions dominate the next stage of the gasification process. In general, the combination of the products from the drying stage, the combustion stage and the pyrolysis stage react together to produce the main final gasification products. These include gas-vapour and gas-solid reactions, which are individually either exothermic or endothermic, some of the notable ones are shown in Equations 6 – 9:

C + CO_2 ⟷ 2CO (Boudouard reaction; ΔH_{298K} = + 172 kJ/mol) (6)

C + H_2O ⟷ H_2 + CO (Water-gas reaction; ΔH_{298K} = + 131 kJ/mol) (7)

CO + H_2O ⟷ H_2 + CO_2 (Water-gas shift reaction; ΔH_{298K} = − 41 kJ/mol) (8)

C + $2H_2$ ⟷ CH_4 (Methanation reaction; ΔH_{298K} = − 75 kJ/mol) (9)

CH_4 + H_2O ⟷ CO + $3H_2$ (Methane steam reforming; ΔH_{298K} = + 205 kJ/mol) (10)

CH_4 + CO_2 ⟷ CO + $2H_2$ (methane dry reforming; ΔH_{298K} = + 124 kJ/mol (11)

The existence of temperature gradient within gasifiers can have significant influence on the final yields of gas products [36]. For instance, due to the chemical equilibrium established during this reduction stage, the endothermic reactions are favoured in the high temperature zones, while the exothermic reactions become dominant in the low temperature zones. While high temperatures can lead to increased oxidation and the reduction in tar formation, it may also lead to the softening and melting (sintering) of the dominant alkali oxides found in biomass ash [37]. Therefore, a careful selection of the temperature of the reduction stage is a key parameter that determines the composition of the gas products and the behaviours of the ash [38].

The use of steam as gasifying agent tends to promote those reactions that involve water (as steam) including Equations 7, 8 and 10. With air or oxygen as gasifying agent, available steam comes from combustion, pyrolysis and possibly the original moisture content of the biomass feedstock. However, there is a complete absence of combustion during steam gasification, so that the steam-based reactions with carbon and methane (Equations 7 and 10) dominate the early gasification reactions, leading to the production of CO and H_2. These equilibrium reactions can influence each other. With increasing concentrations of CO, the water-gas shift reaction (Equation 8) leads to increased H_2 production. For instance, the depletion of CO through Equation 10, can promote its formation through Equations 8 and 10. Hence, steam gasification produces higher H_2/CO ratios in the syngas compared to air or oxygen gasification systems [39].

3.3. Influence of gasifier operating conditions

For gasifier using air or oxygen as gasifying agent, the equivalence ratio, φ (Equation 12) is a key parameter that determines the extent of gasification and hence the yields and compositions of gas products.

$$\text{Equivalence ratio } (\varphi) = \frac{\left(\dfrac{Flow\ rate\ of\ Oxidant_{(actual)}}{Flow\ rate\ of\ Biomass}\right)}{\left(\dfrac{Flow\ rate\ of\ Oxidant_{(stoichiometry)}}{Flow\ rate\ of\ Biomass}\right)} \tag{12}$$

φ can be calculated with either mass or molar flow rates.

Equivalence ratio is used to show the extent of combustion of biomass, and this controls the gasification temperature [40]. More oxidant (air or oxygen) indicates more combustion and hence higher gasification temperature. For gasification, an equivalence ratio of around 0.25 is considered appropriate. φ lower than 0.2 renders excessive tar formation indicating the dominance of the pyrolysis regime (pure pyrolysis occurs at φ = 0). In addition, φ value above 0.45 increases the rate of oxidation (combustion), leading to more carbon dioxide and steam in the product gas, reducing its lower heating value (LHV). Hence, φ values with the 0.2 – 0.45 range are commonly used in air and oxygen gasifiers. For fixed bed gasifiers, using φ values in the upper range may be beneficial, given that the formation of combustion-derived steam can

increase the steam-to-biomass ratio in the reduction zone, which can promote Equations 7, 8 and 10. The influence of the oxidation-generated steam would depend on the temperature at the reduction zone. For instance, higher temperatures would promote both Equations 7 and 10, while a lower temperature would favour Equation 8. Also, higher φ can also increase the Boudouard (Equation 7) and methane dry reforming (Equation 11) reactions, due to increased concentration of CO_2.

For gasification using steam as gasifying agent, the steam-to-biomass (S/B) ratio is the equivalent to φ. Steam gasification occurs around the temperature range of 750 °C - 800 °C and higher S/B ratio leads to higher conversion efficiency of the biomass [41]. This also leads to reduced tar formation, possibly due to higher rate of steam reforming of hydrocarbons under the reaction conditions. As mentioned above, higher S/B ratio promotes Equations 7, 8 and 10, which make significant contributions to the yields and compositions of gas products. Typically, S/B ratios greater than 2.7 have been found to produce consistent gas products with high H_2 contents due to the conversion of CO via Equation 8 [41].

In practice however, steam temperatures are usually lower than the gasifier temperatures, so that S/B ratios much higher than 2.7 would lead to lower gasification bed temperatures, which will promote several exothermic reactions, especially methanation and the formation of other hydrocarbons and organic compounds [10]. S/B ratios below 1.35 lead to higher yields of methane, other hydrocarbon gases and CO_2, while the yield of CO tend to decrease and therefore hydrogen yields are lower compared to S/B > 2.7 [41]. Between these two, S/B ratios ranging from 1.35 to 2.7, favour reactions that produce methane and CO, especially Equations 7 and 9 as well as reverse reactions of Equations 10 and 11 (CO hydrogenation, which can also produce other hydrocarbon gases following Fisher-Tropsch synthesis). A major limitation for the use of steam as gasifying agent is the energy requirements for its generation and maintenance in vapour phase during biomass gasification [42 - 43]. For instance, a simple energy balance calculation would show that generating 1 bar superheated steam at a gasification temperature of 850 °C requires around 5 times the energy needed to heat up dry air from ambient to the same gasification conditions.

In addition, the hydrogen-to-carbon (H/C) ratio used during biomass gasification can influence the concentration of H_2 in the gas product. This is the ratio of all the hydrogen atoms present within the reaction space to the carbon content of the biomass. In this case, all hydrogen atoms within the gasification space include the hydrogen atoms in the biomass, the moisture in the biomass and the steam (if steam gasification). Among these sources of hydrogen atoms listed above, only the hydrogen from steam can be used in practice to manipulate the H/C ratio. Experimental data have shown that an increase in H/C ratio from 1.6 to 2.2 increased H_2 contents in the gas products, indicating increased overall gasification, higher LHV and reduced tar yields (from 18 g/Nm^3 to just 2 g/Nm^3) [44]

Both the temperature of the gasifying agent and the temperature profiles of the gasifier have also been reported to influence the yields and compositions of gas products [45]. Increasing the temperature of the gasifying agent to as close as possible to the gasification temperature can be achieved in practice by using

a pre-heater, which is normally powered by the heat exchanger using the product gas as the heating medium [45]. Using high gasifying agent temperature, avoids temperature reduction across the gasifier profile while decreasing tar and char formation. Higher gasification temperatures at the appropriate φ and S/B ratios, respectively can enhance the gasification efficiency, increase the gas and H_2 yields, thereby giving a gas product with higher LHV [45 - 46]. Experimental data have shown that an increase in gasification temperature from 700 °C to 800 °C increased both H_2 content and carbon conversion efficiency [46]. Under the same conditions, methane, CO and tar contents were found to reduce [46]. Using steam as gasifying agent, an increase in temperature would favour the highly endothermic CO-producing reactions (Equations 6, 7 and 11) and the CO produced is subsequently converted to CO_2 and H_2 via Equation 7. Whereas with air or oxygen as gasifying agent, the early occurrence of Equation 2 would promote mainly Equation 6 due to limited presence of steam. Hence, more CO than H_2 are produced, but the yields of both gases tend to increase with increasing gasification temperature [47], due to a corresponding increased rate of Boudouard reaction (Equation 6).

4. Modelling of biomass gasification

The evaluations of biomass gasification chemistries in *Section 3.2* have mostly resulted from experimental laboratory investigations, during which the effects of various parameters on the yields and compositions of products have been determined. Essentially, gasification experimental designs are accompanied by detailed and often rigorous standardized and novel analytical chemistries for the characterisation of feedstocks and products. The results of these analyses are presented in different ways to explain the predominant reaction mechanisms, the reaction kinetics, and thermodynamics of biomass gasification process, for which a large body of literature have been and are still being published. Data from laboratory investigations provide the basis for explaining the conversion efficiencies of the different gasification technologies.

In contrast, modelling studies can be widely used to predict biomass gasification, without relying on time-consuming and expensive experimental approaches. Over the years, several models for biomass gasification processes have been published using different methodologies and categories [48 – 70]. Table 3 presents some interesting and relevant reviews on biomass gasification modelling published in recent years in Science Direct. These modelling studies are often aimed at the development of more useful methodologies that can provide practical and reliable results. Such studies can identify the most efficient conditions for biomass gasification from First and Second Laws of thermodynamics. For instance, the effect of various operational parameters, such as gasifier temperature, gasifier pressure and air flow rate on the gas product composition and H2/CO was investigated by parametric sensitivity analyses [48]. The results showed that the optimal operating condition to maximize hydrogen and carbon monoxide production were gasifier temperature of 600 °C, gasifier pressure of 1 atm and air flow rate of 0.01 m3/h [48].

Table 3: A selection of relevant reviews on biomass gasification modelling (Science Direct)

Authors	Year	Review Title	Ref
A. Gómez-Barea and B. Leckner	2010	Modeling of biomass gasification in fluidized bed	[49]
M. Puig-Arnavat and J.C. Bruno, A. Coronas	2010	Review and analysis of biomass gasification models	[50]
S.L. Narnaware and N.L. Panwar	2022	Biomass gasification for climate change mitigation and policy framework in India: A review	[51]
T.K. Patra and P.N. Sheth	2015	Biomass gasification models for downdraft gasifier: A state-of-the-art review	[52]
D.C. de Oliveira, E.E.S. Lora, O.J. Venturini, D.M.Y. Maya and M. Garcia-Pérez	2023	Gas cleaning systems for integrating biomass gasification with Fischer-Tropsch synthesis - A review of impurity removal processes and their sequences	[53]
X. Xiang, G. Gong, Y. Shi, Y. Cai and C. Wang	2018	Thermodynamic modelling and analysis of a serial composite process for biomass and coal co-gasification	[54]
Q. He, Q. Guo, K. Umeki, Lu Ding, F. Wang and G. Yu	2021	Soot formation during biomass gasification: A critical review	[55]
M. Costa, V. Rocco, C. Caputo, D. Cirillo, G. Di Blasio, M. La Villetta, G. Martoriello and R. Tuccillo	2019	Model based optimization of the control strategy of a gasifier coupled with a spark ignition engine in a biomass powered cogeneration system	[56]
G.C. Umenweke, I.C. Afolabi, E.I. Epelle and J.A. Okolie	2022	Machine learning methods for modelling conventional and hydrothermal gasification of waste biomass: A review	[57]
Y. Wu, H. Wang, H. Li, X. Han, M. Zhang, Y. Sun, X. Fan, R. Tu, Y. Zeng, C.C. Xu and X. Xu	2022	Applications of catalysts in thermochemical conversion of biomass (pyrolysis, hydrothermal liquefaction and gasification): A critical review	[58]
C. Li and K. Suzuki	2009	Tar property, analysis, reforming mechanism and model for biomass gasification—An overview	[59]
S. Safarian, R. Unnþórsson and C. Richter	2019	A review of biomass gasification modelling	[12]
X. Zhang, A.C.K. Yip and S. Pang	2022	Advances in the application of active metal-based sorbents and oxygen carriers in chemical looping biomass steam gasification for H2 production	[60]
A. Goel, E.M. Moghaddam, W. Liu, C. He and J. Konttinen	2022	Biomass chemical looping gasification for high-quality syngas: A critical review and technological outlooks	[61]
D. Baruah and D.C. Baruah	2014	Modeling of biomass gasification: A review	[62]
M. Mehrpooya, M. Khalili and M.M.M. Sharifzadeh	2018	Model development and energy and exergy analysis of the biomass gasification process (Based on the various biomass sources)	[63]
M.L.Villetta, M. Costa and N. Massarotti	2017	Modelling approaches to biomass gasification: A review with emphasis on the stoichiometric method	[64]

H. Shahbeik, W. Peng, H. K. S. Panahi, M. Dehhaghi, G. J. Guillemin, A. Fallahi, H. Amiri, M. Rehan, D. Raikwar, H. Latine, B. Pandalone, B. Khoshnevisan, C. Sonne, L. Vaccaro, A.-S. Nizami, V. K. Gupta, S. S. Lam, J. Pan, R. Luque, B. Sels, M. Tabatabaei and M. Aghbashlo	2022	Synthesis of liquid biofuels from biomass by hydrothermal gasification: A critical review	[65]
M. Cortazar, L. Santamaria, G. Lopez, J. Alvarez, L. Zhang, R. Wang, X. Bi and M. Olazar	2023	A comprehensive review of primary strategies for tar removal in biomass gasification	[28]
S. Ascher, I. Watson and S. You	2022	Machine learning methods for modelling the gasification and pyrolysis of biomass and waste	[66]
J. Ren, J.-P. Cao, X.-Y. Zhao, F.-L. Yang and X.-Y. Wei	2019	Recent advances in syngas production from biomass catalytic gasification: A critical review on reactors, catalysts, catalytic mechanisms and mathematical models	[67]
M. Ajorloo, M. Ghodrat, J. Scott and V. Strezov	2022	Recent advances in thermodynamic analysis of biomass gasification: A review on numerical modelling and simulation	[68]
I.P. Silva, R.M.A. Lima, G.F. Silva, D.S. Ruzene and D.P. Silva	2019	Thermodynamic equilibrium model based on stoichiometric method for biomass gasification: A review of model modifications	[69]
C.F. Palma	2013	Modelling of tar formation and evolution for biomass gasification: A review	[70]

Some of the most recent reviews have focused on all categories of modelling [50-51,55,57-63,65,28,66-67,69-70]. Other available reviews were orientated towards fluidised beds [49], downdraft gasifier [52], Fisher-Tropsch synthesis [53], co-generation system [56] and thermodynamic equilibrium modelling [54,64,68]. The classical modelling methods reported in the literature are thermodynamic equilibrium (stoichiometric and non-stoichiometric), kinetic and computational fluid dynamics (CFD) [71].

The simplest models consider mass and energy balances across gasifiers to predict the composition of the products, not considering processes and chemical reactions. In this approach, the equilibrium condition is achieved by minimization of Gibbs Free energy and is mostly suitable for various biomass feedstock, whose chemical formulae are unknown (may be obtained from ultimate compositional analyses). The kinetic models are used to predict kinetic mechanisms of the gasification process from gas composition, temperature dependence and the overall gasifier efficiency. The CFD model focuses on analysis of the fluid flow, heat transfer, mass transfer and related system phenomena using numerical methods [71].

Giving the focus of this present review on thermochemistries of biomass gasification, CFD will not be discussed further. Hence, this section of the review will discuss thermodynamic (stoichiometric and non-stoichiometric) and kinetic analysis (Figure 5), which are commonly used for biomass gasification models from the viewpoint of chemical reactions.
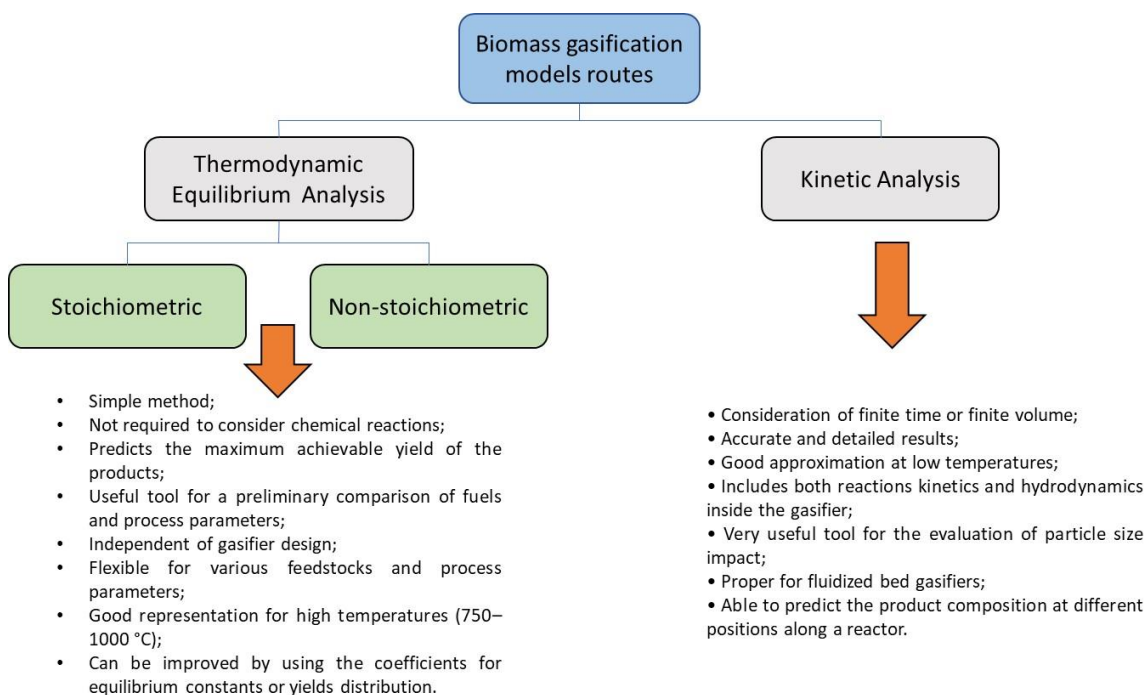
Figure 5: Biomass gasification based on routes processes [3]

4.1. Kinetic modelling of biomass gasification

The kinetic analysis of biomass gasification involves studying the rates and mechanisms of the chemical reactions occurring during the gasification process. Giving the several overlapping reactions that occur

during biomass gasification, kinetic modelling can help to simplify the determination of important kinetic parameters, including activation energy (Ea), towards optimizing the reaction conditions in the gasifier. The advantages of the kinetic models for biomass gasification are to predict performance using mass and energy conservation equations, and to inform the composition of gas products and understand reaction mechanisms, which can aid the optimum design of gasifiers. Kinetic modelling is mostly suited for optimizing and investigating the impact of features such as pore size distribution, feed densities and sensitivity primarily on outgassing flow rate, carbon reduction and system stability. Moreover, it considers kinetic and transport factors that are difficult to find experimentally. While these quantities are evaluated, the resulting models are generally restricted to the feedstocks, gasifier types, gasifying agents, operating conditions, and syngas composition arrangement for which the reaction rates and model parameters are valid.

A large selection of factors can be validated by kinetic models where the equilibrium models cannot. Kinetic models are based on several mechanisms, which explain the chemical processes that occur through the biomass gasification process and are critical in the development, evaluation, and improvement of gasifiers. Kinetic analysis offers the tools to evaluate the progress of the reactions in the gasifier, giving the composition of the products, the distribution of temperature, concentration, and other parameters along the reactor [62]. For example, influence of residence time, type of gasifier, gasifying agent and biomass feeding rate on biomass gasification efficiency can be predicted by kinetic models [63]. Therefore, understanding the effects of gasifier types and gasifying agents on the kinetics of biomass gasification is vital for accurate kinetic modeling of the process. The choice of the gasifier type and gasifying agent can significantly impact the reaction rates, syngas composition, and overall gasification efficiency. Therefore, in-depth research and analysis are essential to optimize gasification conditions and develop reliable kinetic models that can predict the behavior of biomass gasification systems.

4.1.1. Kinetic modelling based on biomass feedstock

Feedstock characteristics play a crucial role in the kinetic modelling of biomass gasification processes. The properties of the biomass feedstock, such as composition, size, moisture content, and ash content, significantly influence the gasification reactions and the overall process performance. The elemental and proximate compositions of biomass provide insights into the chemical structure, heating value, and reactivity of the biomass [49]. Different biomass types exhibit variations in their compositions of carbon, hydrogen, oxygen, nitrogen, and sulfur content, which directly impact the gasification kinetics [49 - 50].

The particle size distribution of biomass affects its heat transfer characteristics, reaction rates, and gasification kinetics. Smaller particle sizes provide larger surface areas for the reactions to occur, resulting in enhanced reactivity. Particle size also influences the mass and heat transfer limitations within the gasifier [51,52]. However, while smaller particle sizes can enhance the reaction rates, they may also increase the gasifier pressure drop and the risk of agglomeration. Furthermore, the moisture content in biomass affects the overall gasification process by influencing the heat requirements, reaction rates, and

gas composition [28]. Higher moisture content can lead to increased heat consumption and lower gasification efficiency [28, 69]. In addition, biomass ash contents have low-melting characteristics, which promote slagging and fouling during gasification, and therefore limit the temperature range for operation. High ash content can lead to agglomeration, bed defluidisation, and corrosion, thereby affecting the gasification kinetics and overall system performance [56,60].

Wang and Kinoshita [72] established a method that predicted the influence process variables such as retention time, reaction temperature, pressure, moisture content, char particle size and equivalent ratio on gas products. Giltrap et al. [73] presented a steady-state model that described the gas-char reactions occurring in a downdraft biomass gasifier. The authors considered some factors such as temperature, pressure, and gas composition to predict the gasification performance and the composition of the produced gas, based on the prevalent pyrolysis and oxidation reactions. In addition, Nikoo and Mahinpey [74] proposed a semi-kinetic model with *Aspen Plus®* for the steady-state operation of the bubbling fluidized bed reactor. These authors used four CSTR reactors to simulate hydrodynamics and heterogeneous chemical reactions of biomass gasification. The calculated rates of CO_2 and H_2 formation were underestimated, even though considerable generation of H_2 was reported at temperatures above 800 °C. However, the authors found that using data generated from experimental thermogravimetric analysis helped to obtain more accurate parameters to support more precise mathematical models to describe the gasification process and reaction mechanisms [74].

4.1.2. Kinetic modelling based on gasifier types

Several authors have worked on the kinetic modelling of biomass gasification based on gasifier types, especially with downdraft gasifiers due to having well-define reaction zones [72 - 73, 75 – 84]. In their study, Wang and Kinoshita [72] developed a methodology that considered critical variables such as retention time, reaction temperature, pressure, moisture content, char particle size, and equivalence ratio. Giltrap et al. [73] utilized the reaction kinetics parameters from Wang and Kinoshita's work to construct a framework but acknowledged that the model's validation was limited as it overestimated methane concentrations. This discrepancy was likely due to the assumption that all oxygen in the air supply was converted to CO_2, disregarding the fact that some methane would react with oxygen during the pyrolysis product cracking process. Additionally, the model did not incorporate the complex pyrolysis and tar cracking processes, comprising various reactions and intermediate products [73].

To address these limitations, Babu and Sheth [76] introduced a variable char reactivity factor to adjust the reaction rates and achieve better consistency with experimental data. They considered the influence of factors like temperature, time, and heating rate on the volatile compounds and gases produced during biomass pyrolysis. Building on this approach, Gao and Li [77] developed a downdraft gasifier model that integrated the pyrolysis and reduction regions to predict temperature and producer gas concentration patterns over time and space [77]. They explored two ways to adjust the temperature of the pyrolysis

zone: using a gas heating rate of 25 °C/min or maintaining a constant temperature of 1127 °C. The simulation results for temperature and gaseous species concentrations closely matched experimental data [77].

Jayah et al. [78] divided their kinetic model into two sub-models, namely: flame pyrolysis and gasification zones. Their objective was to investigate the impact of operating variables such as feedstock moisture levels, chipping size, reactor shielding, ambient temperature, and gasification load on downdraft gasifier performance. The model integrated chemical reaction equilibria with energy and material balance concepts. The gasification zone sub-model utilized inputs from the flame pyrolysis zone sub-model, including calculated temperature and concentrations [78]. Along the vertical axis of the gasifier, a one-dimensional single-particle model was employed in the gasification region sub-model, which considered chemical and physical processes, transport phenomena, flow equations, and conservation principles. The model was calibrated using gas compositions obtained from experiments, and a series of computer simulations were conducted to assess the effects of various operational parameters. It was found that moisture levels and heat loss significantly influenced the reactor's temperature and conversion efficiency. Increasing the length of the gasification zone improved the conversion efficiency for designs with narrower throat angles. While gasifier performance could be enhanced at high intake temperatures, the associated heating costs did not compensate for the gains. The study highlighted the importance of selecting the appropriate gasification zone length for optimal gas production under specific operational parameters [78]. Sharma [79] followed up on this by proposing a kinetic model with separate sub-models for each region, aiming to achieve higher thermochemical processing of biomass into combustible gases (CO and H_2) by optimizing reaction temperatures.

Rabea et al. [84] developed a model for the gasification process in a downdraft reactor and has been validated using experimental data from the gasification of different types of woody biomass and considering various reactor scales and power loads. The predicted results from the model showed a high level of agreement with the experimental data, indicating its reliability. This suggests that the model can be confidently used for sensitivity analysis to predict the performance of a gasifier at different load levels, specifically in the air flow rate range of $3 - 10$ L/s [84]. The authors also explored the impact of the supplied air flow rate on various factors, showing that as the air flow rate increased, the LHV of the gas decreased. In contrast, the gas yield behaved conversely, increasing with higher air flow rates.

Gómez-Barea and Leckner [49], Watson et al. [66] and Gao and Li [80] have all developed kinetic models for fluidized bed gasifiers. Kinetic modelling of fluidized bed gasifiers involves several hypotheses or sub-models, including those for fluidization, gas flow across the fluidized bed, and char conversion under different operating conditions [79]. Reman [81] proposed a model for fluidized bed reactors that treated both gas and solid particles as distinct phases to avoid the complexity of the bed's multiphase nature [81].

However, it is important to note that the existing models for fluidized bed gasifiers still have limitations in fully capturing the behavior of both gas and solid components. Experimental investigations conducted by various contributors, such as Baliban et al. [82], Gomez-Barea et al. [83], and Li et al. [84], focused on specific geometric and operational parameters, providing valuable insights for specific fluidised bed gasifier designs. However, for broader applicability and optimization purposes, it is necessary to establish correlations between input and output parameters based on large datasets to develop a generic model that can accommodate different sizes and operating parameter ranges in fluidized bed gasifiers.

4.1.3. Kinetic modelling based on gasifying agents

The choice of gasifying agent is another crucial factor that influences the kinetics of biomass gasification. Air, oxygen, and steam are commonly used as gasifying agents, each with its own impact on the gasification process and the resulting syngas composition. Air is the most used gasifying agent due to its availability and low cost. However, air gasification has some limitations. As mentioned earlier in *Section 1,* the presence of nitrogen in air dilutes the syngas, reducing its heating value and overall energy content. Moreover, the slower reaction kinetics associated with air gasification can prolong the residence time required for complete conversion of biomass, which otherwise would result in incomplete conversion and the formation of undesirable byproducts, according to the free model developed by Gomez and Mahinpey [85].

Oxygen or a mixture of oxygen and steam can be employed as alternative gasifying agents to enhance gasification kinetics and improve the quality of the produced syngas. The use of oxygen-rich gasification, such as partial oxidation or oxygen-blown gasification, increases the reaction rates, shortens the residence time, and improves the overall gasification efficiency [86]. Oxygen-rich environments promote higher syngas heating values and reduce or eliminate the nitrogen dilution effect. However, oxygen-rich gasifying agent can lead to excessive gasification temperatures, due to the absence of the cooling effect of nitrogen thereby promoting combustion-based reactions. Hence, in most cases, the use of oxygen-steam mixtures as gasifying agents aids in temperature moderation, prevents excessive char oxidation, and enhances hydrogen production [86].

4.1.4. Kinetic modelling based on operating conditions
In-depth research and analysis are essential to optimize operating conditions in gasifiers and develop reliable kinetic models that can predict the behavior of biomass gasification systems. Operating conditions play a crucial role in influencing the gasification kinetics and overall efficiency of the process. Gasification reactions are highly temperature dependent. Higher temperatures generally result in faster reaction rates. However, excessively high temperatures can also lead to undesirable side reactions, such carbon deposition. Different temperature regimes can affect the selectivity of gasification reactions and influence the composition of the resulting syngas [67]. Residence time, which refers to the duration of biomass in the gasification reactor is another important operating parameter. It is critical parameter in influencing

the extent of biomass conversion and the composition of the syngas. Longer residence times generally lead to higher conversion rates but may also promote secondary vapour condensation reaction resulting in tar formation. Shorter residence times can limit the completion of gasification reactions. A complete kinetic-based data on biomass gasification process was calculated and optimized by Dang et al. [87] to evaluate syngas production. The results showed that the initial volatile composition from the pyrolysis step was vital for gas product distribution. The authors also found that the gasification temperature was very sensitive to the syngas composition and yield, followed by the equivalence ratio, S/B ratio, and biomass moisture content [87]. The authors illustrated the effects of two parameters (gasification temperature and syngas yield) and reported optimal syngas yields between 61.4 % and 78.5 % [87].

The kinetics of the pyrolysis stage during biomass gasification were described by Koufopanos et al. [88] using a two-stage model. The initial decomposition of biomass resulted in the formation of volatiles, gases, and char; however, these primary pyrolysis products could further react with char, leading to a range of volatiles, gases, and char with varying proportions. This secondary interaction between the main pyrolysis products altered the distribution of end products [74, 88 - 94]. Babu and Chaurasia [95] solved the pyrolysis equations using the 4th order Runge-Kutta technique across a wide range of conditions, including temperatures from 500 °C to 1500 °C and heat rates from 25 °C/s to 360 °C/s. Their study determined optimal pyrolysis zone parameters, such as temperature, heating rate, and pyrolysis time, under various operating conditions [95].

While kinetic modelling of biomass gasification has contributed to the understanding of biomass gasification, there are still some challenges that must be considered:

- complete reaction mechanisms are frequently unpredictable or are just partially understood.
- kinetic modelling remains highly reliant on reaction rate estimation and more computationally expensive than thermodynamic modelling.
- there are limited research data to deal with the kinetic representation of the sequential order of the process; it is important to consider the sequential order of the gas release from the biomass particles as it moves inside the gasifier through different temperature zones.
- kinetic analysis of the non-condensable gases (CO_2, CO, CH_4 and H_2) needs to be explained based on the non-isothermal nature of biomass gasification.

4.2. Thermodynamic analysis of biomass gasification

Thermodynamic equilibrium equations are simpler compared to kinetic ones and can be stoichiometric or non-stoichiometric (Figure 6). Thermodynamic evaluation of biomass gasification is often aimed at calculating the energy and exergy efficiencies of gas production [42, 93 - 94]. Hence, thermodynamic analysis, is seen as a more appropriate method to study the fuel and thermal process parameters of biomass gasification. The gasifier is computed based on the equilibrium constants (stoichiometric) or

minimization of Gibbs free energy (non-stoichiometric), and the combustor is modelled based on combustion reactions (Equations 2 - 4). Most of the thermodynamic equilibrium models reported in the literature (72.5%) is the non-stoichiometric method [12].
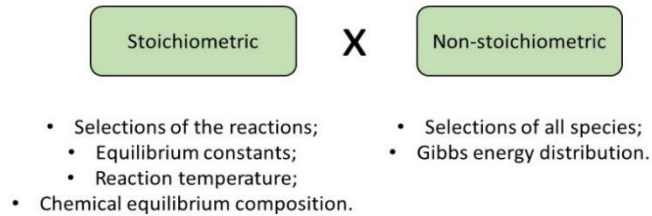

Figure 6: Stoichiometric vs non-stoichiometric models

The Gibbs free energy minimization principle is a fundamental concept in thermodynamics and is often used in equilibrium modelling. It provides a framework for determining the most stable composition of a system at a given temperature and pressure. In the context of gasifiers, the principle suggests that the gasifier reaches its most stable composition when it reaches chemical equilibrium. When a gasifier operates at equilibrium, the entropy is maximized, and the Gibbs free energy (a measure of the system's potential to do work) is minimized. This means that the system has achieved a balance between the reactants and products, and there is no further driving force for chemical reactions to occur. Equilibrium modelling, also referred to as zero-dimensional modelling, aims to predict the final composition of the gasifier based on the minimization of Gibbs free energy [59].

Most of the thermodynamic equilibrium models available in the literature consider the following assumptions [64]:

- Steady state;
- Infinite residence time;
- Ideal gas behaviour of the gas phase;
- Perfect mixing with uniform pressure and temperature;
- The produced gas have no oxygen;
- Nitrogen is inert;
- Potential and kinetic energies are neglected;
- The major species compose the produced gas (H_2, CO_2, CH_4, CO, H_2O and N_2);
- Tar is modelled in the gaseous state;
- Air is sufficient to convert all carbon in produced gas;
- The gasifier operates isothermally and at atmospheric pressure;
- The gasifier is considered adiabatic.

The main parameters that can influence the quality of the produced gas during the gasification process include gasification temperature, biomass moisture content, gasification agent and mass flow rates. Some

thermodynamic studies have focused on some individual parameters, while some have looked at multiple factors at the same time.

4.2.1. Thermodynamic modelling based on feedstock

Feedstock selection directly impacts the overall efficiency, product yield, and environmental impact of the gasification process. Different biomass feedstocks possess unique chemical compositions, moisture contents, and heating values, all of which significantly influence gasification efficiency. By examining the properties, such as moisture content, ash content, elemental composition, and volatile matter content, researchers can determine the optimal operating conditions, adjust process parameters, and develop efficient gasification systems. Additionally, feedstock analysis aids in identifying potential challenges and implementing appropriate pre-treatment techniques to enhance gasification efficiency and minimize operational issues.

Abuadala and Dincer [90] studied the energy and exergy efficiencies of steam gasification of sawdust. The exergy efficiencies were obtained 50% and 69% for hydrogen and all the products, respectively. They found that increasing hydrogen in the steam gasification process depended on the steam mass flow rate, the biomass quality and the operating temperature [90]. Karamarkovic and Karamarkovic [91] studied the effects of biomass moisture contents and gasification temperature using air as the gasifying agent. A thermodynamic evaluation for air biomass gasification was carried out by Zhang et al. [60]. They compared the results with the biomass gasification in the presence of steam and partial oxidation as the gasifying agents which showed production of gas products with higher LHV than that of air. Sharma and Sheith [92] carried out an experimental study on air/steam biomass gasification. The authors established an equilibrium model to predict the performance of the system. The results showed the effects of the steam to biomass ratio and of direct insertion of the steam to the reduction zone on the output gas composition.

4.2.2. Thermodynamic modelling based on gasifier types

Thermodynamic equilibrium models are valuable in the construction and operation of gasifiers because they provide a benchmark for understanding the expected composition of the gas produced. By considering factors such as pressure and temperature, these models can estimate the equilibrium state of the gasifier under various conditions. This information can be useful for optimizing the design and operation of gasifiers, as well as for monitoring process parameters to ensure efficient and stable performance [62]. The findings contribute to the optimization and design of gasification systems for biomass utilization. Modelling based on gasifier types plays a significant role in determining the system's operating principles, reaction pathways, and availability of process parameters. Accurate representation of the gasifier type in models enables better predictions of gasification performance, gas composition, and heating value that can guide decision-making in biomass and waste-to-energy applications.

A numerical approach to estimate gasification in downdraft biomass gasifiers was demonstrated by Melgar et al. [96]. Their model offered simplicity and accuracy in predicting the influence of air/fuel ratios and moisture levels on the composition of production gases. However, it was found that this model tended to overestimate the heating value of CH_4 and H_2 outputs, as well as the amount of CO produced. Zainal et al. [97] presented a study on the use of thermodynamic equilibrium to analyze the biomass gasification process. The authors focused on two pivotal gasification reactions: the Boudouard equilibrium and heterogeneous water-gas shift reactions, along with hydrogenating gasification. The effects of moisture content and reaction temperature on syngas composition and heating value were investigated. When comparing their model to experimental results, it was observed that the model underestimated the quantity of oxygen by specifying it in terms of several elements in the product gases, which was not apparent when compared to the experimental evidence.

Another study conducted by Mountouris et al. [98] involved thermodynamic analyses of plasma biomass gasification. The researchers estimated the gas composition and performed energy-related computations. The findings indicated that increasing airflow in plasma gasification was always unfavorable due to the decrease in H_2 and CO levels, accompanied by an increase in CO_2, N_2 and H_2O levels. Furthermore, it was demonstrated that temperatures above 800 °C led to increased concentrations of CO and H_2O, decreased concentrations of H_2 and CO_2, while the N_2 concentration remained unchanged [98].

4.2.3. Thermodynamic modelling based on gasifying agents and process conditions

Gasifying agents are known to play a crucial role in the energetics of biomass gasification. They control the reaction conditions inside the gasifier [99 - 105], yields and compositions of gas products as well as whether or not tar is formed [99 – 109]. A theoretical comparison of oxygen, oxygen-enriched air, air and steam gasification was carried out by Shayan, Zare, and Mirzaee [89] through thermodynamic model and exergy analysis. The effects of moisture content, gasification temperature and biomass (wood and paper) feeding rate on the process were studied. The results showed that the highest hydrogen production was achieved when steam is used as the gasification agent (gas product calorific value exceeding 11 MJ/Nm^3), followed by oxygen, oxygen-enriched air and air. The results also show that air gasification led to the highest sensible energy efficiency, while steam gasification exhibits the highest exergy efficiency. In addition, they explained that the increase in gasification temperature corresponded to an increase for hydrogen concentration during steam gasification. Furthermore, the model considered the chemical reactions involved in the gasification and allowed for the calculation of equilibrium compositions and thermodynamic properties of the producer gas. The results obtained from the model showed good validation against existing theoretical and experimental data found in the literature [89].

Hosseini, Dincer and Rosen [93] indicated that a greater energy and exergy efficiency results of biomass gasification were achieved in the presence of air as the gasifying agent, instead of the steam gasification.

Schuster et al. presented an extensive study on thermodynamic model for steam gasification, which indicated that gasification temperature and the oxygen content in the fuel had effect on gasification efficiency [100]. Mahishi and Goswami studied energy efficiencies for biomass gasification in air-steam mixtures to investigate the influence on hydrogen production [103]. The authors evaluated the effects of temperature, pressure, SBR and ER parameters on hydrogen yield and it was detected that combined steam and air gasification has produced more H_2 than air gasification. The results showed gasification temperature of 727 °C, SBR of 3, ER of 0.1 and at a gasifier pressure of 1 atm gave efficiency of 54% [103].

Recently, the use of CO_2 and steam-CO_2 or O_2-CO_2 mixtures as gasifying agents for biomass conversion to syngas have been reported [101 - 102]. Vikram et al. studied the thermodynamic analysis and parametric optimization of steam-CO_2 based biomass gasification system using Aspen Plus software to investigate gasification temperature, reaction temperature and gasifying agent composition on H_2 and CO concentration, H_2/CO ratio, and the syngas process efficiency [101]. The energy efficiency of the gasification system was calculated at 900 °C. The Peng-Robinson with Boston Mathias function was selected to simulate the gasification process using both isothermal and adiabatic reactor operations at atmospheric pressure, ideal gas behaviour, ash as an inert material, negligible formation of tar and other heavy hydrocarbons [101].

Renganathan, et al. [102] investigated the gasification process using CO_2, CO_2-steam and CO_2-O_2 as a gasifying agent, syngas composition, cold gas efficiency and CO_2 conversion. The results showed that atmospheric gasification using CO_2 was not favorable under adiabatic conditions. Nevertheless, complete carbon conversion could be obtained by increasing the operating temperature or the CO_2 flowrate [102]. Chaiwatanodom, Vivanpatarakij and Assabumrungrat [90] performed a thermodynamic analysis of biomass gasification with CO_2 recirculation. The results showed that the addition of CO_2 in the gasification process could increase the syngas production only in some ranges of operating conditions (high pressure and low temperature) [104].

Wang, Bi and Wang [105] performed a thermodynamic analysis from biomass gasification for biomethane production based on the minimization of Gibbs free energy. The biomass gasification performance using different gasifying agents (H_2O, CO_2, O_2 or air), was analyzed. The authors showed that steam addition was important to improve carbon conversion and the use of air, O_2 and CO_2 led to a negative impact on the methane yield and H_2/CO ratio. The maximum methane yield was achieved at the temperature at which carbon was completely converted. The authors showed that for the thermodynamic analysis, steam gasification was the ideal conversion process for biomethane production [105].

Avoiding tar is critical to efficient biomass gasification systems so tar modeling is likely to be one of the most active domains of study. Using kinetic mechanism developed by Abdelouahed, et al. [107], Aneke and Wang [117] used Aspen Plus to perform thermodynamic analysis of biomass gasification and the

efficiency of the process was 43.6%. The authors reported that the thermodynamic analysis of biomass gasification process combined with tar removal using plasma technology was efficient for syngas with appropriate tar concentration for gas turbine application [108]. Shamsi et al. investigated a new process to produce hydrogen from lignocellulosic biomass gasification tars using Aspen HYSYS software for the simulation. The authors considered tar reforming and ash separation, combined heat and power cycle, hydrogen sulfide removal unit, water-gas shift reactor, gas compression and hydrogen separation from a mixture of gases in pressure swing adsorption. The results showed that using CHP cycle and plug flow reactor increased the overall energy efficiency (63%) compared to the basic process (29.2%) [109].

In summary, kinetic and thermodynamic modelling of biomass gasification have contributed and will continue to contribute to the optimization and design of gasification systems for improved biomass conversion and quality of the gas product. Accurate representation of the gasification process in modelling enables better predictions of gasification performance, gas composition, and heating value that can guide further optimal development in this area and enhance its contribution towards low-carbon energy production and the achievement of Net Zero.

5. Challenges of tar production and strategies for its reduction during biomass gasification

Among the primary reactions involved in biomass gasification, tar formation is a major bottleneck in biomass gasification, which represents both hazardous operation (fouling and corrosion of gasifier equipment) and lower carbon conversion efficiency. Tar consists of high molecular weight compounds such as single-ring aromatic compounds, oxygenated compounds, polycyclic aromatic hydrocarbons (PAHs) [152] that have formed during the pyrolysis stage of the gasification process and have not been converted to syngas in the gasifier. Primary catalysts have been effective in limiting and controlling the formation of tar during biomass gasification [153], leading to improved H_2 and H_2/CO yields [154 – 155].

Solving the tar problem during biomass gasification would lead to enhanced biomass conversion to gas and improved syngas quality. As already discussed in *Section 2*, significant tar reduction can already be achieved through innovative gasifier designs and operations. This is an active research area with low tar formation being reported from certain large capacity gasifiers such as the conventional fluidized beds [143 - 145], dual fluidized beds [146 - 148], plasma gasifiers [24] and the novel fountain enhanced conical spouted gasifier [149]. In some cases, the type of gasifying agent used during the gasification process can also influence the formation and yield of tar [69, 150 - 151]. Tar removal may also be achieved via a combination of catalysts and physical methods *(Section 6.1)* including hot vapour filtration and the use of condenser. In addition, tar elimination and reduction can be accomplished either inside (*in situ*) or outside (*ex situ*) the gasifier [153]. Each method has its unique influence on effectiveness, catalyst deactivation challenges and process economics.

5.1. Catalytic systems for tar reduction and elimination during biomass gasification

Catalysts help to decrease the required temperature and time for the biomass gasification process for efficient production of high-quality syngas (or producer gas). There are several excellent reviews [27, 65, 70, 75, 125 - 130] and experimental research published on the various catalysts used in biomass gasification [126, 131 - 142]. Biomass gasification catalyst are considered successful if they can lower the required activation energy for gasification reactions to achieve the high carbon conversions that positively influence gasification process. Broadly speaking, biomass gasification catalysts are classified into primary and secondary (downstream) catalysts based on their roles along the conversion process depicted in Figure 7 [110].
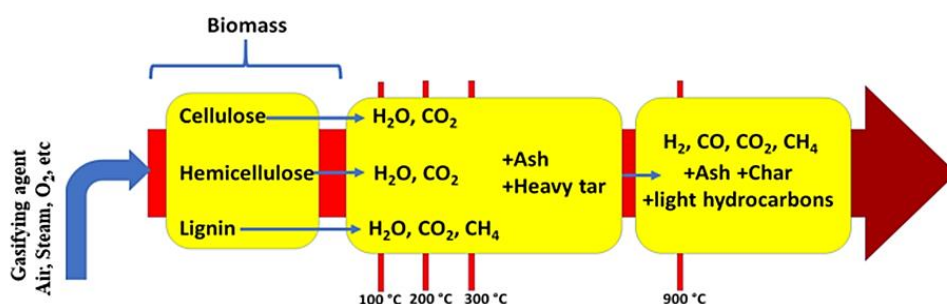

Figure 7: Simplified conversion pathway of biomass gasification

During biomass gasification, primary catalysts alter the reaction pathways to favour the production of high-quality syngas through enhanced reaction rates during the pyrolysis and initial gasification stages [68, 111 - 113]. Such reactions include char gasification (Equation 7) [114 - 115], tar cracking and reforming [121] and the various reactions represented by Equations 2 – 12. In contrast, secondary catalysts are used to promote reactions beyond the main gasification steps. Indeed, secondary catalysts promote the conversion of products of incomplete gasification of the original biomass to enhance the yields hydrogen and CO. Such post-biomass gasification reactions include downstream steam reforming of methane (and other hydrocarbons) in the gas products (Equation 10) [116 - 120], dry reforming methane (and other hydrocarbons) in the gas products (Equation 11) and water-gas shift (Equation 8) [122 - 124].

Tar formation remains a significant challenge to biomass gasification process and there require continued research attention. Tar reduction or elimination via catalysis can enhance biomass conversion efficiency for improved syngas quality. However, for tar conversion, the definition of catalysts as primary or secondary is not clear-cut. In practice, the application of catalyst for tar conversion can be carried out *in situ* (inside the gasifier) or *ex situ* (outside the gasifier). Hence, technically, materials used for *ex situ* catalyst systems for tar conversion may be referred to as secondary catalysts as they do not influence the reactions within the gasifier. In contrast, *in situ* catalytic systems have the potential to influence both the gasification reactions (including preventing tar formation) as well as subsequent conversion of gas phase products (including the reforming of formed tar). Hence, materials for *in situ* catalysis can promote both primary and secondary reactions. Therefore, this present review has focused on the *in situ* and *ex situ*

positioning catalysts systems for eliminating or reducing tar formation. In some cases, a combination of catalytic systems for primary gasification and secondary reforming of tars have been report [121, 128, 173].

5.1.1. Catalysts for ex situ tar reduction and elimination during biomass gasification

Catalysts are usually employed for *ex situ* tar removal over a temperature range of 600 °C to 900 °C and should be capable to reform hydrocarbon gases and the aromatic compounds and heavy organic compounds that are present in tar. The main catalyst selection criteria include cost, catalytic activity, efficiency, deactivation and sulphur poisoning resistance, stability, environmentally friendly, easy regeneration, reusability, and mechanical strength [112, 127, 156 – 157]. Furthermore, materials for tar conversion can be grouped into synthetic and naturally occurring catalysts. Among these, natural minerals, alkali metals, transition metals, and noble metal-based catalysts have been reported to be most effective with promising results. Alkali metals (Ca, Na, and K), alkali-metal based catalysts, as well as heavy metals are reported as the most suitable and effective catalysts [159]. Fluid catalytic cracking (i.e., zeolite) catalysts, alkali-metal based catalysts, activated alumina, and transition-metal based catalysts (Ni-, Pt-, Zr-, Rh-, Ru-, and Fe-based catalysts) are grouped as the synthetic catalysts. Natural/mineral catalysts include calcinated rocks (calcite, magnesite, and calcinated dolomite), olivine, clay minerals, and ferrous metal oxides [149, 158]. Studies have also reported waste by-products including char, derived from thermochemical processing of biomass and solid organic products, as reliable, low cost, sustainable alternative to the commercially available catalysts [160].

Ex situ catalytic systems for tar reduction or elimination have recently combine both catalytic cracking and with physical methods such as hot vapour filtration [161], to reduce energy composition via heating and cooling cycles and to convert tar into syngas and to increase the gasification efficiency [161 - 163]. These hot gas catalytic filters have found practical application for tar reforming, ammonia elimination and particulate elimination [164] during biomass gasification. Catalytic filters are either presented as a solid fixed catalytic bed or a cylindrical filter candle with catalytic foam coating inside. Catalytic coating on the inner tube has been found to be more cost effective in terms of manufacturing costs. Silicon carbide, a wood-derived ceramic material, was described as a suitable filter material due to its high thermal stability at temperatures above 750 °C [165]. The main drawback of hot filtration vapour devices is the limited surface area availability for application of catalytic coating, which directly affects the interaction between the filter walls and catalyst leading to lower efficiency and stability of the coating. To obtain a uniform and stable coating containing active metals, studies suggested deposition of catalyst coating with urea [166].

Several researchers have reported the effectiveness of low-cost biomass-derived char (biochar) as catalyst for *ex situ* conversion and reduction of tar [167 - 173]. For example, the adoption of a two-stage gasification process, with a primary gasifier and a secondary reformer, have been reported to improve biomass conversion efficiency and product gas quality by using char as a catalyst in the secondary

reformer to reduce tar concentrations in the product gas [121, 128, 173]. The effectiveness of char for tar removal depends on its properties such as surface area, pore volume, and surface functional groups, and the operating conditions such as temperature, pressure, and gas compositionThe catalytic activity of char can be further enhanced through impregnation of active metals [174]. High surface area and porosity of the char surface, allow and supports impregnation of active metal particles through a simple dry mechanical mixing. Specifically, biochars have desirable porous structure and contains valuable minerals mostly on its surface, which enhance the catalytic behaviour of the char towards tar conversion and gasification reactions [175]. Biomass naturally contains alkali and alkaline earth metallic species (AAEMs) including K, Na, Ca, Mg, which generally benefit gasification process through tar cracking and reforming of tar. These AAEMS also provide additional resistance to carbon deposition and sintering [176 - 177] by being a good hosting matrix for impregnated metal catalyst, thus promoting excellent interaction and contact between active metal particles and tar. The presence of minerals, porous structure of char is another advantage in providing a suitable hosting matrix. However, high ash content of biochar can lead to fouling, clogging, and slagging throughout the gasification process. Excess AAEMs in biochar can be removed via selective acid leaching and aqueous washing to remove unwanted components and to promote development of the porous structure [178].

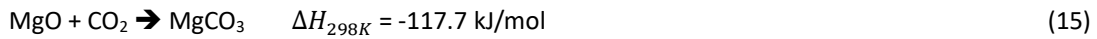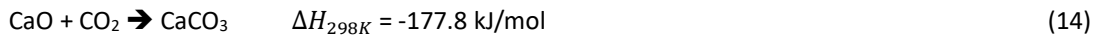### 5.1.2. Catalysts for in situ tar reduction and elimination during biomass gasification

In contrast to *ex situ* systems, *in situ* treatment involves placing the catalyst inside the reactor for tar conversion or to suppress its formation. During in situ catalysis, the catalyst material may be mixed with or completely replace the usual bed materials (silica sand). *In situ* tar treatment has been reported to be more than *ex situ* promising in terms of tar removal following direct interaction of catalyst with volatiles [179]. The main catalyst selection criteria include cost, catalytic activity, efficiency, deactivation and sulphur poisoning resistance, stability, sustainable source, ease of regeneration, reusability and mechanical strength [180]. In addition, catalysts that are employed for *in situ* tar conversion or suppression must be able to withstand the gasifier conditions. For all types of gasifiers, the *in situ* catalyst must withstand the high gasification temperatures (800 – 1000 °C) and specifically, for fluidized beds, these catalysts must have the added mechanical strength to withstand the fluidization conditions (particularly, high gas velocities and potentially high rates of attrition) inside the gasifier.

Natural materials such as dolomite ($CaMg(CO_3)_2$) , limestone ($CaCO_3$) and olivine ($(MgFe)_2SiO_4$) are cheap and abundant catalysts for tar reduction and elimination and they are recommended to be employed as bed material in fluidized bed gasifiers [122, 181]. These natural catalysts can be used directly or after pre-treatment. However, natural catalysts have their own drawbacks, including particle fragmentation, moderate activity rate, and relatively low catalytic activity towards reforming of hydrocarbons [160]. For instance, unlike olivine, dolomite and limestone have poor attrition resistance and therefore suffer severe particle fragmentation in fluidized bed gasifiers [182].

Dolomite is a naturally occurring mineral, introduced as *in situ* catalyst during gasification to achieve enhanced syngas yield with up to 95 % tar removal [183]. They have also been found to be highly effective in the gasification of PAHs components of tar [184]. Often, dolomite is pre-treated by calcination before use according to Equation 13:

$$CaMg(CO_3)_2 \rightarrow CaO + MgO + 2CO_2 \qquad \Delta H_{298K} = +296 \text{ kJ/mol} \qquad (13)$$
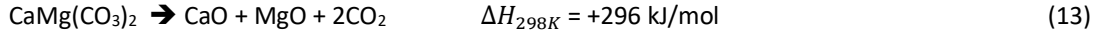
Calcined dolomite is also effective in enhancing hydrogen yields during steam gasification within the temperature range of 750 °C to 850 °C [183]. The sorption-enhanced yield of hydrogen is promoted by altering the position of equilibrium of water-gas shift reaction (Equation 8) through the removal of CO_2 by the oxides (Equations 14 and 15), which represent the reverse of Equation 13.

$$CaO + CO_2 \rightarrow CaCO_3 \qquad \Delta H_{298K} = -177.8 \text{ kJ/mol} \qquad (14)$$

$$MgO + CO_2 \rightarrow MgCO_3 \qquad \Delta H_{298K} = -117.7 \text{ kJ/mol} \qquad (15)$$

Studies reported up to 14 % increase in gas production with notable reduction in tar yield using calcined dolomite [143]. During air gasification of rice husk, increase in dolomite quantity from 10 to 40 %, increased hydrogen, carbon oxide, and carbon dioxide yield from 2.6 to ~4 %, 15.2 to 17.3 %, and 9.3 to 10.5 %, respectively [185]. Hydrogen content from gasification of cotton stalk chops using dolomite, olivine, and quartz sand was reported as 31.45, 23.72, and 22.79 %, respectively [186], showing the superior performance of dolomite. Furthermore, hydrogen yields from gasification of cellulose [144], spruce wood pellets [187], pine saw dust [188], almond shell [145], bark pellets [150], refuse-derived fuel (RDF) [189], using calcined dolomite were reported to be 8.33, 22.80, 49.33, 55.5, 25.8, and 13 %, respectively. In addition, as the calcium and magnesium carbonates (or oxides, in calcined form) are alkaline, they provide added benefits through their involvements in acid-base reactions to remove acid gases such as HCl and SO_2 in the gas products [151].

Compared to the amorphous dolomite, crystalline dolomite with bigger pore structure was reported to provide better mechanical strength as it allowed swift release of gas [151]. However, gasifier operations at high temperatures (>850 °C), often result in a more porous and fragile structure of dolomite, which directly affects the mechanical strength of the catalyst, thereby limiting the number of their effective catalytic cycles [157].

Olivine ($(MgFe)_2SiO_4$) is another well-known abundant naturally occurring mineral being used as a catalyst during biomass gasification [145, 150, 186, 189]. As an in-bed additive, the advantages of olivine over silica sand and dolomite are its durability, tar elimination activity, and strong abrasion (anti-wear) resistance during biomass gasification [150, 189]. Reduction in tar content (~42 %) was reported with an increase in olivine quantity from 10 to 40 % [185]. Similar to the dolomite, calcined olivine (pre-treated at 900 °C and above) can provide better catalytic properties for improved tar cracking, due to the migration of iron to the olivine surface [171] . Calcination at 1100 °C increased tar conversion by 55.9 % [190]. To further improve olivine tar cracking and elimination, studies have suggested impregnation of olivine using

active metals; Fe/olivine [191], Ni/olivine and Ni-Ce-Mg/olivine [192], Cu/Ni/olivine [180] and Ni/olivine/La_2O_3 [193]. Such added metals have been found to enhance catalytic activity by providing more active sites when used *in situ* during biomass gasification [180, 191 – 193].

The CaO contents in limestone and dolomite have been reported to be responsible for effective cracking and elimination of tar. Therefore, the direct use of CaO as another cheap and widely available biomass gasification catalyst has been variously explored [116, 194 – 202]. Application of CaO is notable for obtaining higher hydrogen yield at lower temperatures (~600 °C) [116] through the combination of Equation 7 and 13, shown in the exothermic Equation 16 below.

$$CaO + CO + H_2O \rightarrow CaCO_3 + H_2 \qquad \Delta H_{298K} = -220.8 \text{ kJ/mol} \qquad (16)$$
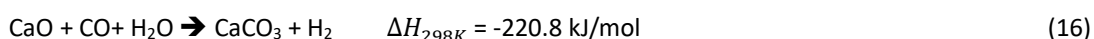
For example, increasing CaO/biomass mass ratio from 0 to 2, increased hydrogen concentration in the gas product from 23.29% to 54.54 % during gasification of White fir. Moreover, under similar reaction conditions, hydrogen yield increased from 34.5 to 59.1 % during the gasification of sawdust [195 - 196]. Hydrogen content of gas composition based on gasification of sawdust [190], corn stalk [145], rice straw [145], pine sawdust [197], pine sawdust [198], wood [199], soft wood [200], larch [201], almond shell [202], using CaO catalyst in the gasifier, was reported to be 54.43%, 61.23%, 60.28%, 52, 57%, 48%, 70.3%, 63.56%, and 55.5 % respectively. In addition, CaO has also been reported as an effective tar cracking catalysts when used as at high temperatures (~800 °C) [116].

Meanwhile, alkali metal-based catalysts (especially, the hydroxides and carbonates) are known to provide relatively higher yields of hydrogen, higher hydrocarbon reforming efficiency and advanced tar cracking and removal ability [111, 146 – 147]. Indeed, the presence of alkali catalyst permits desirable tar cracking at higher temperature as (up to about 1300 °C) [111]. Yet, alkali metal catalysts are expensive, produce a notable amount of ash, and are not recommended to be employed as *in situ* catalysts at temperature higher than 800 °C [113]. Hence, the main drawback of alkali metal catalysts arises from the low melting points of these metals leading to their vaporisation at elevated temperatures, condensation and agglomeration on cooler surfaces after exiting the gasifier, leading to eventual clogging of pipes [202]. These alkalis can be employed either directly (mixed with biomass) or impregnated with another catalyst [146]. Among the alkali metal-based catalysts, KOH has been most widely used due to its relatively higher impact on the biomass gasification efficiency. For instance, in comparison with other alkali metal-based catalysts (NaOH, K_2CO_3 and Na_2CO_3), the use of KOH led to reduced tar content and improved hydrogen yield during the gasification of sewage sludge [147].

Transition metal-based catalysts, especially those of nickel, are suitable to be employed as *in situ* catalysts, and provide comparably enhanced catalytic activity, good tar reforming efficiency, higher hydrogen yield, and complete tar elimination [203]. They are considered highly active in steam reforming process within a temperature range from 500 °C to 950 °C. However, nickel-based catalysts are not recommended for use in fluidized beds due to the poor attrition resistance. Also, their deactivation behaviour and poor sulphur poisoning resistance is another drawback. This deactivation has been linked to the formation and
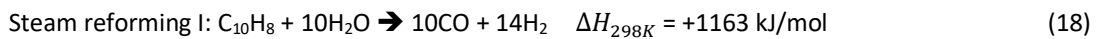
agglomeration of dust and coke deposits on the catalyst active surface, thereby blocking the pores and active sites [204]. Studies suggested support materials, including zeolites, dolomite, olivine and metal oxides to minimize the challenges of using nickel-based catalysts [113, 117, 123, 127, 156, 157, 205]. For example, the application of olivine as a support material for nickel-based catalyst enhanced its mechanical strength, tar destruction (up to 94%), hydrogen generation (up to 56% vol%), and was considered a suitable material to improve catalytic bed recirculation [113, 117, 127]. Moreover, studies recommended chemical modification of catalyst using basic elements including K, Na, Mg and Fe [156, 205,].

Due to the challenges of poor longevity of nickel-based catalyst s due to deactivation, poor attrition resistance and sulfur poisoning, researchers have investigated the use of other transition and d-block metals for tar elimination during biomass gasification [199 - 200]. These include application of Rh, Ru, Pd, Pt, Co, Zn, Cu and Fe, resulting in a relatively higher tar removal, higher stability, and lower carbon deposition as compared to the Ni-based catalysts [199]. While these non-nickel catalyst are considered highly practical and effective for tar elimination, the platinum-group metals (PGMs) are highly expensive and have negative impacts on processing costs [118].

5.2. Catalytic mechanisms and performance

Tar decomposition involves several simultaneous reactions including thermal decomposition, steam and dry reforming and water-gas shift. A basic catalytic mechanism involves the dehydrogenation of compounds in tar on active sites of catalysts. Thermal decomposition can lead to carbon formation, leading to carbon deposition on catalysts active sites as well, which have the potential to react with steam to generate additional CO and preserve catalytic activity [203]. Studies on the catalytic mechanism of tar cracking have relied on the use of model compounds. Due to the complex composition of real tar, benzene, toluene, naphthalene, and sometimes tetradecane or furfural have been mainly employed as model tar compounds to better understand the catalytic mechanism [125, 206].

Using naphthalene vapour (gas phase) as tar model compound [186], its conversion reactions could be presented as the idealised Equations 17 – 20 as follows:

Cracking: $C_{10}H_8 \rightarrow 3C_2H_2 + 4C + H_2$ $\qquad \Delta H_{298K} = +531$ kJ/mol $\qquad$ (17)

Steam reforming I: $C_{10}H_8 + 10H_2O \rightarrow 10CO + 14H_2$ $\quad \Delta H_{298K} = +1163$ kJ/mol $\qquad$ (18)

Steam reforming II: $C_2H_2 + 2H_2O \rightarrow 2CO + 3H_2$ $\qquad \Delta H_{298K} = +35.6$ kJ/mol $\qquad$ (19)

Dry reforming I: $C_{10}H_8 + 10CO_2 \rightarrow 20CO + 4H_2$ $\qquad \Delta H_{298K} = +1575$ kJ/mol $\qquad$ (20)

Dry reforming II: $C_2H_2 + 2CO_2 \rightarrow 4CO + H_2$ $\qquad \Delta H_{298K} = +118$ kJ/mol $\qquad$ (21)

Carbonisation: $C_{10}H_8 \rightarrow 10C + 4H_2$ $\qquad \Delta H_{298K} = -150$ kJ/mol $\qquad$ (22)

Apart from Equation 22, all the potential equations for tar conversion range from being mildly to highly endothermic, confirming why tar reforming is usually more effective at high temperatures. Therefore, tar conversion mechanism can further be explained through three main stages using naphthalene. These include (1) initial endothermic (Equation 17) and exothermic decomposition (Equation 22) to lower hydrocarbon gases, carbon and hydrogen gas; (2) subsequent moderately endothermic reactions for the conversion of the small hydrocarbons through steam (Equation 19 and 21); and (3) consumption of carbon through Boudouard reaction (Equation 6) and water-gas reaction (Equation 7). These reactions are much more favourable than the highly endothermic steam (Equation 18) and dry (Equation 20) reforming of naphthalene itself [207].

In addition, catalytic mechanism studies based on model tar compounds (tetradecane, toluene and naphthalene) showed that through thermal decomposition, straight-chained hydrocarbons converted to shorter hydrocarbons, whereas aromatic hydrocarbons were predominantly converted to benzene, which easily formed carbon [208]. In a recent study, Shao et al. [163], reported that naphthalene resulted in higher formation of carbon as compared to toluene using nickel-based catalyst. This observation was linked to the 2-ringed structure of naphthalene. Higher char bed temperature and residence time (up to 900 °C for 15 min) were found more effective in conversion of naphthalene, which agree with the high endothermic nature of the main conversion reactions.

5.3. Catalyst deactivation mechanisms during biomass gasification

Despite the many benefits in using catalysts in biomass gasification, there are several drawbacks which require precise studies and attention. These include catalyst deactivation by various mechanisms including thermal, physical and chemical processes as shown in Figure 8 [119]. In addition, thermal or chemical catalyst deactivation is directly influenced by the nature of the catalyst, reaction parameters and condition, and biomass characteristics. Often, noticeable decrease in hydrogen yield is mainly the initial sign of catalyst deactivation [117]. Physical deactivation processes including crushing or attrition and fouling leading to loss of morphology and poor structure. Thermal and chemical deactivation processes include coke deposition, catalyst sintering and sulfur poisoning and often lead to reduced surface catalytic surfaces and loss of surface functionalities. Thermally and physically deactivated catalysts are more difficult to regenerate than those that have been chemically deactivated. For example, coke formation is a major challenge during the use of dolomite leading to blockage of active pores, which reduce the catalyst efficiency [160] but may be regenerated via calcination or carbon burn-off. In contrast, regeneration of thermally or physically deactivated catalyst may require rudimentary chemical synthesis. Therefore, this review has focused on the mechanisms of chemical deactivation.
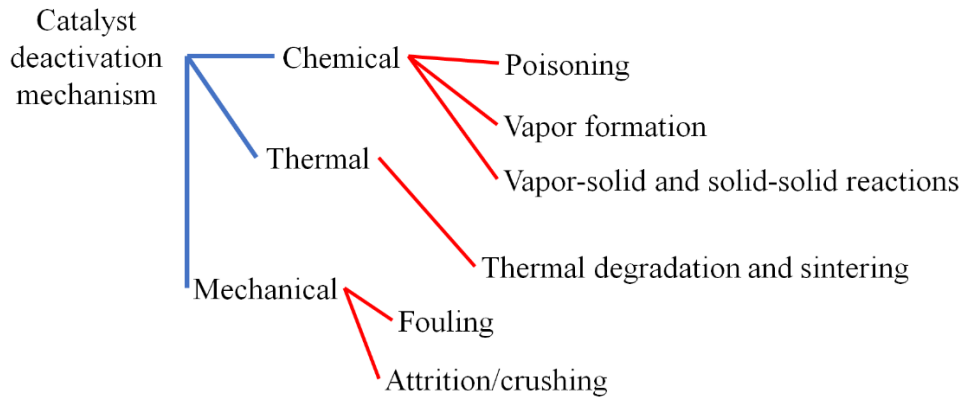
Figure 8: Mechanism of catalyst deactivation

Chemical deactivation process is often magnified in the presence of PAHs and absence of hydrogen donors [209]. For example, as shown in Equations 17 and 22, naphthalene decomposition can cause catalyst deactivation by depositing coke on active sites of the catalyst [120]. Catalyst deactivation requires a rapid response, either by treatment or replacement. Studies suggested increase in the gasification temperature to possibly prevent or at least slow down the coke formation [210]. Meanwhile, for a catalyst like dolomite, high temperature operations are not suitable, as it undergoes fragmentation, deformation, and decomposition at ~600 °C, transforming into fines and dust which can clog the gasifier nozzles and pipelines [211]. Nickel-based catalysts are known for their quick deactivation due to relatively high propensity for carbon deposition, carbon encapsulation, regeneration difficulties, and sintering at high temperatures [212 - 213]. To delay deactivation of nickel based catalysts, studies suggested several treatments and modifications such as alloying with other transition metals, doping with alkali metals, or employing appropriate support materials [203].

Catalyst deactivation has negative impacts on energy consumption, waste generation and process costs. Therefore, the development of durable, readily available, and affordable composite catalysts that are highly active even at low temperatures is highly recommended. As a result of these perspective, studies have shifted their focus towards enhancement of biochar and biochar-based catalysts for biomass gasification [167 - 173, 214].

5.4. Catalyst regeneration methods

Coke formation and deposition result in catalyst deactivation by blocking and covering active sites and pores of catalysts [215]. As a result, regeneration of deactivated catalyst is a crucial process to remove coke and restore catalyst activity. Restoring and regeneration process of deactivated catalyst is based on the catalyst type, deactivation mechanism, coke nature, and regeneration technique. Residual coke formation change during oxidative regeneration (from aliphatic to aromatic), can result in a more complex

process. The selection of regeneration temperature is crucial due to the impact of high temperatures on catalyst form and morphology (sintering) [119]. As a result, it must be noted that regeneration affects catalyst lifetime, and therefore, stable catalyst after repeated regeneration cycles are more desired. As a result, regeneration methods based on lower or at least balanced temperatures, with high efficiencies are more desired. The frequency of catalyst regeneration is directly linked to the coke formation rate and a gasification process with rapid coke formation, requires continuous catalyst regeneration [216].

Regeneration heat effect could be either exothermic or endothermic depending on the type of the employed gas. Regenerations based on air, O_2, O_3, NO_x, and H_2 are exothermic while regenerations based on CO_2, and H_2O are endothermic [148]. Regeneration techniques are oxidation (air, ozone and oxynitride), gasification (carbon dioxide and water steam), and hydrogenation (hydrogen). Oxidation based on air or oxygen (O_2, and O_3) is the most common technique to regenerate catalysts. This technique has been employed in other industrial processes including fluid catalytic cracking, hydrotreating, catalytic reforming, and methanol to olefins processes [129]. The main products of oxidation process include H_2O, CO_2, and CO. The main drawback of oxidation process, is emission of large amounts of CO_2 and the possible oxidation of reduced metal components of catalyst to their oxides, requiring further reduction to restore the initial activity. In addition to oxidation and gasification, recent studies have introduced pyrolysis using inert gas, as well as hydrocracking using hydrogen or alkanes [130].

As mentioned earlier, coke oxidation is an exothermic reaction, and it directly affects catalyst properties at high temperatures. Reduction in temperature is highly desired during coke oxidation to avoid catalyst thermal damage. Otherwise, high temperatures can result in dealumination, metal sintering, and catalyst decomposition. Moreover, it was found that the coke deposited on metal was easier to remove and required shorter regeneration time, and lower regeneration temperature compared to the coke formed on the support materials [217].

Oxidation with O_2 needs to be carried out at temperatures of 500 °C and above. To perform an effective coke removal at lower temperature (50 –200 °C) with a low risk of thermal degradation of catalyst, studies suggested oxidation with O_3 over O_2 due to its strong oxidizing properties [219]. Meanwhile, extensive application of O_3 is limited in industrial processes and it is known for its rapid dissociation on storage. In addition to O_3, NO_x are economical and effective oxidation agents that have the potential to remove coke at low temperatures [218]. While further research is needed, NO_x has been reported to degrade and cause catalyst damage over the oxidation cycles [219].

As an alternative to oxidation process, to reduce CO_2 emission and improve CO production, regeneration of catalyst through gasification using H_2O or CO_2 was found beneficial [220]. For gasification of biomass and sewage, studies reported utilization of CO_2 to be more beneficial following the global warming and carbon footprint concerns [221]. CO_2 has the potential to act as a mild oxidizing agent [182]. Gasification with CO_2 is more preferred than steam gasification as it is a gas, requires no vaporization prior to gasification, and results in weaker damages on catalyst at higher temperatures. However, the rate of

steam gasification of char is 2 – 5 times higher than that with CO_2. Like the oxidation technique, gasification with CO_2 and H_2O are promising methods and can be enhanced using metal additives. Application of metal additives during gasification, improves the process rate and lowers the process temperature. Application of selected metals such as La, Ce, Zn, Ti, and Mn improved gasification rate by 50 – 150% and halved the regeneration time [114]. Low reactivity of CO_2, stability of catalyst, and high process temperature requirement (above 700 °C), are the main drawbacks and concerns of gasification with CO_2 [222].

Moreover, air is generally used in industrial processes, as moderate regeneration temperature can be applied to regenerate deactivated catalyst. Ozone and oxynitride are effective but are harmful gases and cause environmental damages. Regeneration kinetic studies (based on the catalyst active sites), synthesis of thermally stable biomass-based regeneration agents that can improve product selectivity, as well as applicability of different metals in lowering the regeneration temperature, can be recommended for future studies.

6. Underpinning chemistries of the uses of biomass-derived product gas for green chemical production

Syngas or producer gas can be directly combusted to produce power and heat, which is not the focus of this present review. The gas products from biomass gasification are also a resource for the production of various chemicals including hydrogen, methanol, dimethyl ether, fuel-range liquid hydrocarbons and waxes through a variety of chemistries. In this section, the chemistries of the conversion of syngas to organic chemicals are reviewed. While hydrogen production is a major use of syngas via water-gas shift reaction of CO, many reviews on this topic already exists in literature [103] and so, this has not been covered here.

6.1. Downstream tar and particulate matter removal before gas product usage

Even with the most efficient tar cracking catalyst, the eventual product gas still requires cleaning to remove breakthrough tars and particulate matter prior to gas utilization. These impurities are often removed by mechanical and physical techniques [161 – 163]. The techniques involve either an absorption or adsorption process. Absorption was reported to be more effective in heavy tar removal processes, while adsorption technique was found more beneficial in light tar removal processes [223]. Such techniques are optimized according to the downstream application of the gas products. The techniques are identified either as wet gas cleaning system or dry gas cleaning system [224].

Wet gas cleaning system requires liquid scrubbers (venturi, impingement, and packed bed scrubbers), and spray towers, while organic filters, bag filters, and cyclone separators are employed in dry gas cleaning system. Efficiency of liquid scrubber system depends on the amount of soluble tar, and is generally recommended for average sized plants [225]. Wet gas cleaning system is considered expensive as it requires water as the primary scrubbing medium. To overcome this concern, studies suggested application of oil scrubbers (vegetable and waste cooking oil scrubbers) in cyclone scrubbers which resulted in 95.4 % tar removal through pyrolysis of rice husk [226]. Furthermore, wet system discharges a large amount of contaminated water including tar, which requires further treatment as high level of contamination can cause clogging [107, 227]. Application of dry packed bed filters based on biomass materials was found effective after wet scrubber system stage. This included filters based on coconut coir, waste tea, rice husk, fly ash, biochar, wood chips, and saw dust [228].

6.2. Syngas quality requirements and removal of light chemical impurities

Syngas composition strongly depends on the type of feedstock and gasification agents. As an example, Thao et al. [229] conducted air gasification of rice straw, which produced H_2: 5–9 vol%, CO: 14–17 vol%, CO_2: 32–37 vol%, CH_4: 3–4 vol%, C_xH_y: <1 vol%, N_2: 34–36 vol%, and trace pollutants such as HCl and H_2S. Broer et al. [230] conducted steam/oxygen gasification of switchgrass, resulting in a gas composition with H_2: 15–25 vol%, CO: 30–35 vol%, CO_2: 30–45 vol%, CH_4: 5–15 vol%, C_xH_y: 1–5 vol%, N_2: 2–10 vol%, and trace pollutants such as HCN and NH_3. Various technical applications of syngas usually require strict gas composition. Therefore, the direct use of syngas is unrealistic. Therefore, syngas pre-treatments, such as H_2/CO modification ratio and the removal of excess N_2, O_2, CO, CO_2, and trace pollutants from the produced syngas are mandatory.

Syngas is the main chemical synthesis resource to make methanol, dimethyl ether (DME) hydrocarbons, and hydrogen from biomass. The required quality of the syngas strongly depends on the process. For methanol synthesis, the syngas composition must satisfy the stoichiometric number of the methanol formation reaction from H_2 and CO. An $H_2/CO = 2$ is a stoichiometric number for methanol production, however, an excess of H_2 is provided in the syngas to avoid side product formation in industrial processes [231]. For methanol synthesis, CO_2 works as a reaction promoter and the content must be maintained at approximately 2–10 vol% in the feed gas [232]. Sulfur, mainly H_2S, must be kept below 1.6 ppm to avoid catalyst deactivation [233]. An industrial-scale DME production process consists of two steps: the first step is for methanol synthesis and the second step is dehydration of methanol to produce DME. The main drawback of the two-step DME process design is the high energy consumption required for cooling the contact gas to extract methanol and the subsequent heating of the methanol stream prior to entering the DME reactor. Therefore, one-step syngas-to-DME production is an attractive way to avoid interposed cooling and heating steps. The equipment implementation of the DME reactor system is similar to that of the methanol reactor system. The Fischer-Tropsch synthesis for hydrocarbons production requires more

strict removal of impurities as follows [233]: H_2S + COS + CS_2 (<1 ppmv), NH_3 + HCN (<1 ppmv), HCl + HBr + Hf (<10 ppmv), and S, N, and O containing organic components (<1 ppmv). For the use of syngas as a hydrogen source in the industry, high H_2 concentration ($\leqq 98$ vol%) with low concentrations of CO and CO_2 (10–50 ppmv), O_2 (100 ppmv), and others such as hydrocarbons and N_2 (< 2 vol%) is required.

There are several active commercial plants utilising natural gas or syngas worldwide. Those plants are equipped with gas cleaning facilities. The Rectisol™ process employs methanol as an absorbent and is able to capture CO_2, COS, H_2S simultaneously [234]. Conversely, a drawback of this process is the high cost of the chilling process to prevent absorbent loss. The Selexol™ process uses dimethyl ether of polyethylene glycol as an absorbent, which results in negligible absorbent loss owing to its low vapour pressure. The selectivity of the H_2S removal is higher than CO_2 which can lead to efficient removal of both gases [216]. A drawback of this process is the high selectivity of H_2S, which reduces the CO_2 removal efficiency when high amounts of H_2S are present. The Purisol™ process utilises N-methyl pyrrolidone as an absorbent for H_2S and CO_2. This process is also highly effective in removing H_2S as well as the Selexol™ process. This high affinity towards H_2S also causes a hindrance to CO_2 absorption when the H_2S level is high. In addition, another drawback of this process is comparatively high vapour pressure of the solvent, which is prone to absorbent loss [235].

6.3. Synthesis of alcohols from syngas

Alcohols such as methanol, ethanol, and long-chain alcohols have been used as fuels and chemicals. Although their calorific value is lower than that of conventional fuels such as gasoline and diesel, combustion of alcohols is easier than that of conventional fuels owing to the presence of oxygen in the structure. Therefore, they are used directly as fuel or octane-enhancing fuel additives [236]. Furthermore, alcohols are directly used as fine chemicals, or they are common platform chemicals and precursors for further synthesis.

Synthesis of long-chain alcohols through catalytic conversion of syngas derived from biomass is a promising method to accelerate carbon neutrality and can avoid competition between food and energy production. Most syngas catalytic conversion for alcohol synthesis technologies is still at the laboratory stage and catalyst development with higher activity and selectivity is the current primary interest of this field [237]. For alcohol synthesis from syngas, catalysts must have dual functions, i.e. dissociative adsorption and non-dissociative adsorption [238]. According to the reaction process shown in Figure 9, [239 - 240] CO in the syngas is adsorbed dissociatively on the catalyst for forming C* and O*, where C* is hydrogenated to CH_x*. If CH_x* further reacts with CH_x* on the catalyst, the carbon chain is extended. Alternatively, non-dissociated CO* and CH_x* can react together to form acyl species (CH_xCO*), and it undergoes further hydrogenation to form long-chain alcohols. For this process, alkane, alkene, aldehydes, and ester productions are undesired side reactions.

To achieve the high yield and selectivity of long-chain alcohols, a variety of bimetallic catalysts, which have dissociative activation and non-dissociative insertion of CO abilities, have been investigated. According to the literature survey by Khan et al. [241] it can be concluded that the CO conversion and product selectivity strongly depends upon the catalyst performance, which is determined by calcination and activation conditions, active metal species, metal loading amount, and support metal. There are a variety of catalysts, whereas Cu-based catalysts are believed to be the most attractive catalysts among them because they can be further improved to achieve high activity and selectivity by alloying with iron.

Xiao et al. [242] (Entry 1) synthesized unsupported Cu-Fe alloys with different Cu/Fe ratios of 10.00. 3.00, 0.33, and 0.11, and their performances were compared with those of physical Fe and Cu nanoparticle mixtures. The highest alcohol selectivity (26.2 C%, R-OH distribution: R = C1: 15.9 wt%, C2: 9.1 wt%, C3: 6.0 wt%, C4: 8.9 wt%, C5: 9.0 wt%, and C6+: 51.0 C%) with 20.8% CO conversion was obtained by using the Cu/Fe = 3 catalyst (3Cu1Fe) from syngas (H2/CO = 2) at 220 °C at 6 MPa. Conversely, the physical mixture of them showed 13.5 C% selectivity with a comparable 19.4% CO conversion.

$$C_{n+1}H_w$$
$$C_nH_{2n},\ C_nH_{2n+1} \xleftarrow{\ H^*\ } C_nH_z \xrightarrow{\ CO^*\ } C_nH_zCO^* \xrightarrow{\ H^*\ } C_{n+1}H_{2n+3}OH$$
$$\uparrow CH_x^*$$
$$\vdots$$
$$C_2H_4,\ C_2H_6 \xleftarrow{\ H^*\ } C_2H_x^* \xrightarrow{\ CO^*\ } C_2H_yCO^* \xrightarrow{\ H^*\ } C_3H_7OH$$
$$\uparrow CH_x^*$$
$$CH_4 \xleftarrow{\ H^*\ } CH_x^* \xrightarrow{\ CO^*\ } CH_xCO^* \xrightarrow{\ H^*\ } C_2H_5OH$$
$$\uparrow H^*$$
$$C^* + O^* \xrightarrow{\ H^*\ } H_2O^*$$
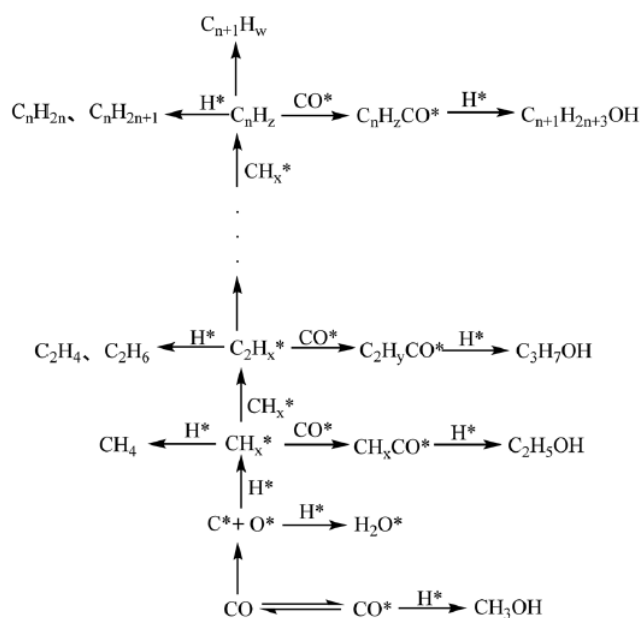$$CO \rightleftharpoons CO^* \xrightarrow{\ H^*\ } CH_3OH$$

Figure 9: The reaction process of CO hydrogenation catalysed synthesis of low-carbon alcohols [243 - 244]

A better CO conversion of 39.5% was reported by Bin et al. [245] by employing a SiO$_2$-coated CuFe catalyst (CuFe@SiO$_2$) with Cu/Fe = 1 at 280 °C at 4 MPa (Entry 2). They concluded that the better CO conversion was due to the higher surface area and pore volume, and the formation of a large amount of CuFe$_2$O$_4$, which leads to strong interactions between copper and iron. Furthermore, the alcohol selectivity was only 7.8%. Fang et al. [246] significantly improved CO conversion to 95% at 300 °C at 3 MPa by employing a Cu-Co bi-metal catalyst, which was prepared from 7.5 wt% CuO/LaCoO$_3$ perovskite (Entry 3). The alcohol selectivity was 31%. The prepared catalyst allowed higher Cu dispersion, which significantly enhanced the Co reduction, and stronger interactions between Cu and Co ions in LaCoO$_3$ particles led to bi-metallic Cu-Co particles formation in the catalyst.

Zhang et al. [247] (Entry 4) synthesized plasma-promoted Fe-Cu bimetal catalyst (FeCuSi-PC). Plasma treatment facilitated the exposure of active Cu and Fe components on the catalyst surface. The synthesized FeCuSi-PC catalysts achieved the maximum 60.2% CO conversion with comparatively high 52.4% alcohol selectivity at 300 °C at 5 MPa. Recently, Li et al. [248] achieved a high CO conversion of 53.2% with an alcohol selectivity of 29.8% at 260 °C at a surprisingly benign reaction pressure of 1 MPa by employing Fe_5C_2-Cu interfacial catalysts (Entry 5). That catalyst was prepared from a $Cu_4Fe_1Mg_4$-layered double hydroxide precursor. Fe_5C_2 clusters (~2 nm) were immobilised onto the Cu nanoparticles (~25 nm) surface. They concluded that the unique interfacial structure of ultrasmall Fe_5C_2 clusters (CO dissociation and subsequent C–C bond propagation) over Cu nanoparticles (CO does not dissociate) achieved the suitable construct for the production of long-chain alcohols production at syngas pressure as low as 1 MPa.

Table 4: Alcohol synthesis, DME synthesis and Fisher-Tropsch synthesis using heterogeneous catalysts
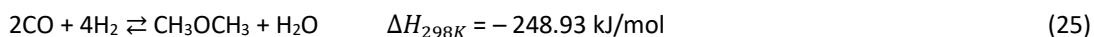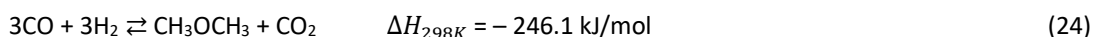
			Alcohol synthesis				
Entry	Catalyst	CO conversion (%)	Alcohol selectivity (%)	Hydrocarbon selectivity (%)	Temperature (°C)	Pressure (MPa)	Reference
1	3Cu-1Fe	20.8	26.2	71.1	220	6	[242]
2	$CuFe@SiO_2$	39.5	7.8	58	280	4	[245]
3	Cu-Co bi-metal catalyst	95	31	-	300	3	[246]
4	FeCuSi-PC	60.2	52.4	33.3	300	5	[247]
5	Cu4Fe1	53.2	29.8	40.2	260	1	[248]
			DME synthesis				
Entry	Catalyst	CO conversion (%)	DME selectivity (%)	MeOH selectivity (%)	Temperature (°C)	Pressure (MPa)	Reference
6	AF1+ XNC-98 (1:2)	87	58	10	250	4	[249]
7	MSC6+SA95 (1:1)	61	95	4	230	8	[250]
8	CZA/NSFER	69	97	-	270	5	[251]
10	CuZnAl/SAPO11-PhyC	92	90 (C-mol%)	9 (C-mol%)	250	2	[252]
	Pd/ZnO-γ-Al_2O_3	31	65	2	270	5	[253]
			Fischer-Tropsch synthesis				
Entry	Catalyst	CO conversion (%)	C_{1-4} selectivity (%)	C_{5+} selectivity (%)	Temperature (°C)	Pressure (MPa)	Reference
11	Co/Al_2O_3	50	8	92	210	2	[254]
12	Co/Al_2O_3	99	21	79	230	2	[254]
13	$Ru/Co/Al_2O_3$	88	24	76	200	2	[255]
14	Al_2O_3-modified mesoporous Co_3O_4	90	12	88	230	2	[256]
15	Co/MMS	92	11	83	220	2	[256]

6.4. Synthesis of dimethyl ether from syngas

Dimethyl ether (DME) is one of the promising alternative fuels for automotive engines, fuel additives, and home cooking gases to replace diesel and liquified petroleum gas (LPG). Currently, DME is synthesized exclusively by a two-step process of methanol production from syngas followed by dehydration of methanol according to the following reaction equations (23 – 25):

$$2CH_3OH \rightleftarrows CH_3OCH_3 + H_2O \qquad \Delta H_{298K} = + 6.91 \text{ kJ/mol} \qquad (23)$$
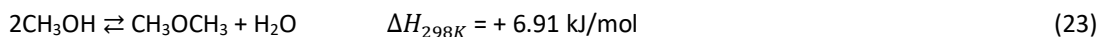
On the other hand, DME can also be produced directly from syngas, consecutive synthesis of methanol and methanol dehydration. The following two reactions are known as direct processes:

$$3CO + 3H_2 \rightleftarrows CH_3OCH_3 + CO_2 \qquad \Delta H_{298K} = - 246.1 \text{ kJ/mol} \qquad (24)$$

$$2CO + 4H_2 \rightleftarrows CH_3OCH_3 + H_2O \qquad \Delta H_{298K} = - 248.93 \text{ kJ/mol} \qquad (25)$$

The reaction (13) requires $H_2/CO = 1.0$, while the reaction (14) needs $H_2/CO = 2.0$. Both the reactions are exothermic and reduce the number of moles, so direct DME synthesis is generally favored by low temperature and high pressure. Therefore, bifunctional catalysts that include CO hydrogenation sites and methanol dehydration sites are very important for this process.

Xia et al. [249] focused on γ-Al$_2$O$_3$ because of its lower cost and less generation of byproducts. However, the acidity of it is not strong enough for methanol dehydration in the syngas-to-DME process. Therefore, the acidity of γ-Al$_2$O$_3$ was modified by fluorination using ammonium fluoride (NH$_4$F) solution with various concentrations. The best dehydration performance was obtained by the catalyst (AF1) which was fluorinated by 0.1 mol/L NH$_4$F solution. The AF1 and a commercial methanol synthesis catalyst (XNC-98: CuO/ZnO/Al$_2$O$_3$) were mixed together with the mass ratio of AF1: XNC-98 = 1: 2, resulting in the highest 87% CO conversion and 58% DME selectivity at 250 °C at 4 MPa.

Takeguchi et al. [250] synthesized a methanol-synthesis catalyst (MSC5: Cu : ZnO : Al$_2$O$_3$: Cr$_2$O$_3$: Ga$_2$O$_3$ = 38.1 : 29.4 : 13.1 : 1.6 : 17.8 (wt.%)) by uniform-gelatin method. The MSC5 and Pd/Al$_2$O$_3$ catalysts were mixed together with the ratio of MSC5: Pd/Al$_2$O$_3$ = 10: 1, resulting in MSC6. In addition, a silica-alumina catalyst (SA95: Silica content = 95 wt%) was prepared by the mechanochemical activation method. The 1:1 mixture of MSC6 and SA95 showed the highest DME yield (58%) with a good selectivity of 95% thanks to Brønsted acid sites with moderate acid strength of the prepared catalysts.

Jung et al. [251] synthesized bifunctional Cu-ZnO-Al$_2$O$_3$ (CZA)-incorporated ferrierite zeolite (FER). They synthesized three different FERs such as needle-like, nanosheet, post-treated mesoporous, and commercial plate-like FERs having a similar Si/Al molar ratio of ~10. CZA nanoparticles on these FERs showed different catalytic activities and stabilities due to the different Cu nanoparticles dispersions with oxidation states as well as hydrophobicity of the FERs. Among them, the needle-like nanosheet FER incorporated with CZA (CZA/NSFER) showed the maximum CO conversion of 69% with a DME selectivity

of 97% at 270 °C at 5 MPa. In addition, the deactivation of CZA/NSFER was not so significant by preventing thermal aggregations of Cu nanoparticles on the hydrophobic NSFER surfaces. The more hydrophobic NSFER contributed to suppress H_2O adsorption.

Phienluphon et al. [252] developed a new physical coating method (PhyC) without employing hydrothermal synthesis way to prepare a new core-shell-like zeolite capsule catalyst named CuZnAl/SAPO11-PhyC catalyst, which has a $Cu/ZnO/Al_2O_3$ (CuZnAl) core catalyst and a PhyC-prepared silicoaluminophosphate-11 (SAPO-11) shell. This catalyst showed 92% CO conversion and 90% DME selectivity at 250 °C and comparatively low pressure of 2 MPa. The excellent catalytic performance of this catalyst provided a confined reaction field to syngas to DME reaction and at the same time suppresses the further deep dehydration of DME to form other hydrocarbon by-products.

Gentzen et al. [253] focused on Pd-based intermetallic compounds to improve methanol synthesis selectivity and thermal stability of the catalysts. They synthesized Zn-stabilized Pd colloids with a size of 2 nm served as the key building blocks for the methanol active component in bifunctional $Pd/ZnO-\gamma-Al_2O_3$. Most notably, the Pd-based catalysts showed excellent stability over time on stream, with CO conversion and DME selectivity remaining constant after 270 h. Higher thermal stability of the intermetallic PdZn compound and higher hydrogenation activity of Pd may prevent particles sintering and deposition of carbonaceous species.

6.5. Fischer-Tropsch synthesis for hydrocarbons

Light olefins including ethylene and propylene, and long-chain hydrocarbons are the most important basic chemicals for a wide variety of products such as plastics and solvents. Currently, petroleum is the primary source of these light olefins. Fischer-Tropsch synthesis is a promising way to produce those chemicals from biomass-derived syngas, which can reduce petroleum-derived carbon consumption and accelerate to achieve carbon neutrality. Fischer-Tropsch synthesis catalytically combines CO and H_2 at 200–350 °C at 2–4 MPa to obtain hydrocarbons. The reaction temperature and pressure are comparable with alcohol synthesis from syngas, while Co-based catalysts are often employed for the reaction owing to a good reactivity balance and price [257]. In general, two major mechanisms, *carbide* and *CO insertion*, are believed to be progressed. The carbide mechanism is progressed through CO direct and H-assisted dissociation. Then, hydrogenation of CO forms dominant monomers CH_x species. The chain growth is progressed via coupling of monomer species (Figure 2(a)). The CO insertion mechanism is progressed via reduction of adsorbed CO and subsequent hydrogenation to alkane or alcohol (Figure 2(b)), whereas Liu et al. [258] concluded that the CO insertion mechanism is less favoured compared to the carbide mechanism.

(a) Carbide mechanism
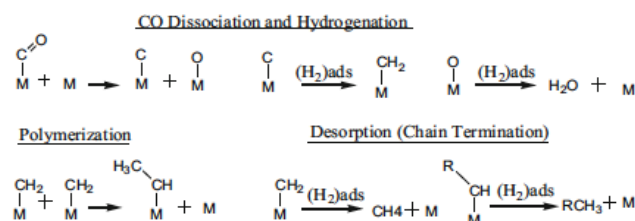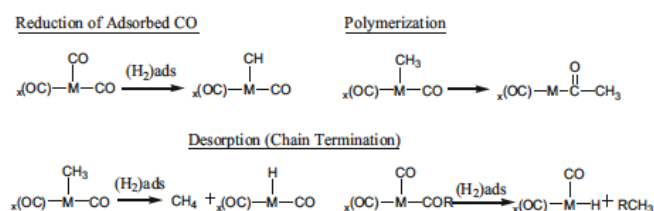

(b) CO insertion mechanism

Figure 8: Fischer-Tropsch synthesis: (a) Carbide mechanism and (b) CO insertion mechanism. [259] Copyright (2014) with permission from Springer [License number: 5510081149408]

Jung et al. [254] synthesized 20 wt% Co loaded γ-Al_2O_3 catalyst, which showed 50% CO conversion at 210 °C at 2 MPa from syngas from H_2/CO = 2. The selectivity of C_{5+} hydrocarbons is very high (92%). When the reaction temperature increases to 230 °C, the CO conversion reached 99%, whereas the C_{5+} selectivity decreased to 79%. Thus, the temperature strongly influenced the CO conversion and chain length of the hydrocarbons. Hong et al. [255] tested a Ru/Co/Al_2O_3 catalyst by impregnation method. Comparatively high CO conversion (88%) was achieved at a comparatively low temperature of 200 °C. Liuzzi et al. [257] reported that bimetallic Ru-Co/Al_2O_3 allowed the formation of small Ru particles deposited at the surface of Co one surface. It is known that the catalytic activity of Ru for hydrocarbons production by Fischer-Tropsch synthesis is higher than that of Co, while a drawback of the Ru is the higher price compared to Co.

Koo et al. [256] simultaneously achieved comparatively high CO conversion (90%) and C_{5+} hydrocarbons selectivity (88%) by employing an ordered-mesoporous Co_3O_4 catalyst. The structural collapse of mesoporous Co_3O_4 was successfully prevented by pillaring Al_2O_3. The high reactivity was achieved by the formation of the strongly interacted Al_2O_3-Co_3O_4 with the spinel-type $CoAl_2O_4$ structures. They also synthesized Co-impregnated hierarchically spherical and ordered meso-macroporous silica (Co/MMS). It has a high surface area (405 m^2/g) with a bimodal pore size distribution, which facilitated the transport of molecules with a larger confining capacity for heavy hydrocarbons inside the regular macropores of the Co/MMS. The CO conversion reached 92% and 83% selectivity of C_{5+} paraffins at 220 °C at 2 MPa from syngas with H_2/CO = 2 [256].

6.6. Applications of hydrogen in energy

Currently, hydrogen energy initiatives are in full swing worldwide. There have been several hydrogen booms to date, but practical applications have not been implemented owing to high cost and immature technology. However, as global warming increasingly progresses, countries worldwide have declared that they will realise carbon neutrality by 2050, and to accomplish this, it must be universally recognised that hydrogen energy utilisation is indispensable. Hydrogen plays an important role in decarbonisation in the power generation sector. Power generation efficiency is higher in fuel cells on a small scale, but the cost performance is better than the fuel cells if the power generation scale is significant. In particular, in the power generation sector, mixed combustion with natural gas is possible, and it is advantageous that the existing thermal power generation equipment can be used. When natural gas and hydrogen are co-fired or hydrogen is exclusively fired, the flame properties change owing to the fuel component changes [260]. Because hydrogen has a higher combustion rate than natural gas, the risk of the flashback phenomenon becomes higher compared to the case of burning only natural gas. Therefore, it is necessary to achieve low NOx and stable combustion, focusing on the improvement of combustors for hydrogen gas turbines to suppress the occurrence of flashback [261]. Specifically, it is necessary to mix hydrogen and air in a narrow space in a short time to avoid high hydrogen concentrations. For example, Mitsubishi Hitachi Power Systems Ltd., has developed a combustor with a large number of nozzles, called a multi-cluster combustor, as a hydrogen-only combustion combustor, and is developing a mixing method that disperses flame and ejects finer and smaller fuel particles [115].

Reducing CO_2 emissions is a major issue even in the steel industry. Efforts are progressing to use hydrogen as a reducing agent for iron ore in blast furnaces [262 - 263], which can contribute to reduce the use of coke as a reducing agent. Regarding the use of hydrogen, hydrogen vehicles are attracting significant attention. Currently, Electric Vehicles (EV) are leading the way in the electrification of vehicles, but it takes time to charge, and it is necessary to install numerous storage batteries to alleviate power shortage in large vehicles that require power. Conversely, hydrogen vehicles (FCV) do not need to be equipped with multiple fuel cells. Therefore, there is a strong opinion that FCVs are suitable for trucks and buses that carry heavy loads over long distances. Hydrogen fuel is being applied not only to FCVs but also to forklifts, railways, ships, and airplanes. As fuel cells for automobiles, polymer electrolyte fuel cells (PEFC) with excellent starting characteristics and power generation output density are chiefly used. The operating principle of hydrogen PEFC is that hydrogen ions (H^+) and electrons (e^-) are generated from hydrogen by catalytic action at the anode (fuel electrode) (hydrogen oxidation reaction (HOR)), and the hydrogen ions move to the cathode (air electrode) by dropping the electrolyte membrane and the electrons reach the cathode via an external circuit. At the cathode, water is produced by oxygen in the air, hydrogen ions and electrons (Oxygen reduction reaction, ORR). The continuous occurrence of this reaction acts as a mechanism that transfers electric current to the outside.

Ambitious research has been investigated to exploit highly active and low-cost catalysts for PEFCs. The primary cost factor of PEFC is the high usage of Pt that is employed for both the cathode and anode. In

general, cathode materials contribute more to the overall cost. Hence, the development of economical and high-performance ORR electrocatalysts is one of the most important factors to reduce the cost of the fuel cell. Carbon-supported Pt group metal nanoparticles are the most widely used catalyst category for PEFC. Now, improvement of the catalyst durability, i.e., avoiding dissolution, sintering/agglomeration, and detachment of the platinum group metal, is a significant challenge in this field [260].

One solution for improved stability and reducing cost is the synthesis of Pt metal alloys. Greeley et al. [261] revealed better ORR activity of binary alloys, Pt_3Sc and Pt_3Y, than single metal Pt. The stability of Pt_3Sc and Pt_3Y resulted from the approximately half-filled metal-metal d bonds and their negative formation energy. Liang et al. [264] synthesized ultrasmall and structurally ordered tetragonal $L1_0$-PtM (with a Pt:M ratio of 1:1) with a few percent of metals (W, Ga, Zn) doping. $L1_0$-W-PtCo/C catalyst, which includes Co and Was the second and third metals, respectively, achieved high activity and stability in the PEFC after 50 000 voltage cycles at 80 °C. They concluded that W doping not only stabilises the ordered intermetallic structure but also tunes the Pt-Pt distances in such a way to optimize the binding energy between Pt and O intermediates on the surface.

Another strategy for stability improvement is the development of advanced catalyst supports. Highly graphitised carbon materials (carbon nanotubes, carbon nanofibers, and graphene oxide, etc.) can improve the intrinsic thermal and chemical stability over that of conventional carbon black [265]. Recently, Qiao et al. [266] developed highly stable porous graphitic carbon produced via pyrolysis of a 3D polymer hydrogel (crosslinked polyaniline (PANI) and polypyrrole (PPy)) in combination with Mn. PANI is rich in aromatic structures, and abundant carbon and nitrogen sources help direct conversion to graphitised carbon [267]. By adding pyrrole, highly folded and contorted graphitic structures with high uniformity and porosity can be produced from a PANI–PPy composite [268]. This support allowed uniform Pt nanoparticle dispersion and enhanced corrosion resistance owing to the good balance of graphitisation and hierarchical porosity.

Non-carbon support materials can perfectly avoid electrochemical corrosion of carbon during long-term operation. Metal oxides such as TiO_2 [269] and NbO_2 [270] prevented catalyst activity decay compared to the conventional Pt/C catalyst. Thus, these works demonstrated huge potential to replace carbon as support to stabilise Pt nanoparticles, while most metal oxides suffer from the impediments in poor electrical conductivity and low surface area. Recently, Xu et al. [271] developed a carbon/metal hybrid support, $CNT-Ti_3C_2T_x$ (1:1), which has metallic conductivity, large surface area, rich surface functional group, and high electrochemical stability.

7. Conclusions

This review has specifically focused on the thermochemistry of biomass gasification, including the main chemical reactions that occur in the gasifier to produce syngas or producer gas. Extensive literature search on various aspects of the gasification process and the downstream chemical processing of gas products have been carried. The use of thermodynamic and kinetic parameters to help with the understanding of the gasification process has been thoroughly reviewed. Considerably, this review has highlighted the differences in the sequence of reactions with respect to the gasifying agent and the type of gasifier. In the presence of limited amounts of oxygen (pure oxygen or air), the reactions involve initial combustion of the biomass to produce a limited amount CO_2 and steam with immediate depletion of oxygen. This creates the right conditions for pyrolysis reactions to dominate to produce species that are cable of reacting with CO_2 and steam. These species include carbon, carbon monoxide and hydrocarbon gases. These pyrolysis products then undergo redox reaction reactions with CO_2 and water to produce the final products of gasification, namely CO and hydrogen.

The use of catalysts to enhance the gasification process has focused on the formation and reduction of tars, which remain a major bottleneck that affects conversion efficiency as well as gas product compositions and yields. The use of natural (olivine, dolomite, calcium oxide, etc.) and synthesized transition metal-based and alkali metal catalysts have been discussed. In addition, the main catalyst deactivation mechanisms and regeneration processes are discussed. Finally, the main uses of gas products (particularly, syngas) for chemical synthesis are discussed, focusing of the production of green methanol, dimethyl ether and longer chain hydrocarbons. The requirements for syngas cleaning and conditioning prior to the synthesis of these chemicals have been reviewed, followed by an extensive review of the different catalytic routes for the conversion of syngas to these compounds. The chemistries of biomass gasification as a source of renewable hydrogen and its utilisation have also been covered. Overall, topic of biomass gasification is continuously gaining attention, with an exponential increase in related research publications. The renewed acknowledgement of bioenergy contributions to achieving Net Zero is arguably a strong driving force.

Overall, the continued research into the chemistries of biomass gasification and its potential applications in a variety of different industries is likely to play a key role in the ongoing transition to a more sustainable and low-carbon economy. As the world continues to shift towards more renewable sources of energy, the use of biomass gasification as a source of renewable hydrogen and other fuels and chemicals is likely to become increasingly important and may help to pave the way for low-carbon energy future to help achieve Net Zero by 2050 and beyond.

8. Acknowledgements

9. Bibliography

[1] J. Popp, Z. Lakner, M. Harangi-Rákos and M. Fári, *Renewable and Sustainable Energy Reviews*, 2014, **32**, 559-578.

[2] Global bioenergy statistics 2020, world bioenergy association. 201210 WBA GBS 2020.pdf (worldbioenergy.org).

[3] Biomass explained - U.S. Energy Information Administration (EIA).

[4] A. Al-Rumaihi, M. Shahbaz, G. Mckay, H. Mackey and T. Al-Ansari, *Renewable and Sustainable Energy Reviews*, 2022, **167**, 112715.

[5] V.C. Pham, B.-S. Rho, J.-S. Kim, W.-J. Lee and J.-H. Choi, *J. Mar. Sci. Eng.* 2021, **9**, 1072.

[6] M. Shahbaz, A. AlNouss, I. Ghiat, G. Mckay, H. Mackey, S. Elkhalifa and T Al-Ansari, *Conservation and Recycling*, 2021, **173**, 105734.

[7] A. AlNouss, G. McKay and T. Al-Ansari, *Journal of Cleaner Production*, 2020, **242**, 118499.

[8] J. van de Loosdrecht, F.G. Botes, I.M. Ciobica, A. Ferreira, P. Gibson, D.J, Moodley, A.M. Saib, J.L. Visagie, C.J. Weststrate. and J.W. Niemantsverdriet. Fischer–Tropsch Synthesis: Catalysts and Chemistry. In: Jan Reedijk and Kenneth Poeppelmeier, editors. Comprehensive Inorganic Chemistry II, 2013, 525-5577. Elsevier, Oxford, United Kingdom.

[9] C. Calin-Cristian, *Energy*, 2023, **270**, 126926.

[10] A.T. Hoang, Z. Huang, S. Nizetic, A. Pandey, X.P. Nguyen, R. Luque and V.V. Pham, I*nternational Journal of Hydrogen Energy*, 2022, **47**, 4394-4425.

[11] S. Mishra, R.K. Upadhyay, Materials Science for Energy Technologies, 2021, **4**, 329-340.

[12] S. Safarian, R. Unnþórsson and C. Richter, *Renewable and Sustainable Energy Reviews,* 2019, **110**, 378-391.

[13] K. Chojnacka, K. Mikula, G. Izydorczyk, D. Skrzypczak, A. Witek-Krowiak, K. Moustakas, W. Ludwig and M. Kułażyński, *Journal of Cleaner Production*, 2021, **320**, 128706.

[14] C. Maurer, J. Müller, *Energies* 2019, **12**, 1294.

[15] J. Havlík, T. Dlouhý, *Chem Engineering,* 2020, **4**, 18.

[16] W-H. Chen, B-J. Lin, Y-Y. Lin, Y-S. Chu, A.T. Ubando, P.L. Show, H.C. Ong, J-S. Chang, S-H. Ho and A.B. Culaba, *Progress in Energy and Combustion Science*, 2021, **82**, 100887.

[17] S. Ma, Y. Yan, C. He, Z. Li, X. Tang, J. Sperry, Y. Sun, L. Lin and X. Zeng, *Industrial Crops and Products*, 2022, **180**, 114712.

[18] J.L. Klinger, T.L. Westover, R.M. Emerson, C. .Williams, S. Hernandez, G.D. Monson and J.C. Ryan, *Applied Energy*, 2018, **228**, 535-545.

[19] D. Serrano, A. Horvat, E. Batuecas and P. Abelha, *Renewable Energy*, 2022, **200**, 1438-1446.

[20] A. Rafey, K. Pal, A. Bohre, A. Modak and K.K. Pant, *Catalysts* 2023, **13**, 420.

[21] A. Pitkäoja, J. Ritvanen, *Energy*, 2023, **266**, 2023, 126446.

[22] S.M. Santos, A.C. Assis, L. Gomes and C. Niobre, P. Brito, *Waste,* **2023**, 1, 140-165.

[23] X. Yang, S. Wang and Y. He, *Renewable and Sustainable Energy Reviews*, 2022, **154**, 111832.

[24] P-C. Kuo, B. Illathukandy, W. Wu and J-S. Chang, *Bioresource Technology*, 2020, **314**, 123740.

[25] S.H. Samadi, B. Ghobadian, M. Nosrati and M.Rezaei, *Fuel*, 2023, **333**, Part 1.

[26] P. Kumar, P.M.V. Subbarao, L.D. Kala and V.K. Vijay, *Chemical Engineering Journal Advances*, 2023, **13**, 100431.

[27] NNFCC Project 09/008. Review of Technologies for Gasification of Biomass and Wastes, Final report, June 2009.

[28] M. Cortazar, L. Santamaria, G. Lopez, J. Alvarez, L. Zhang, R. Wang, X. Bi and M. Olazar, *Energy Conversion and Management*, 2023, **276**, 116496.

[29] V.S. Sikarwar, M. Zhao, P. Clough, J. Yao, X. Zhong, M.Z. Memon, N.S.E.J. Anthony and P.S. Fennell, *Energy Environ. Sci.*, 2016, **9**, 2927–3304.

[30] R. Kumar, V. Strezov, H. Weldekidan, J. He, S. Singh, T. Kan and B. Dastjerdi, *Renewable and Sustainable Energy Reviews*, 2020, **123**, 109763.

[31] A. Ayol, O.T. Yurdakos, A. Gurgen, *International Journal of Hydrogen Energy*, 2019, **44**, 17397-17410.

[32] A. Molino, S. Chianese, D. Musmarra, *Journal of Energy Chemistry*, 2016, **25**, 10-25.

[33] S. Katyal, K. Thambimuthu and M. Valix, *Renewable Energy*, 2003, **28**, 713-725.

[34] R. Xiao, B. Jin, H. Zhou, Z. Zhong and M. Zhang, *Energy Conversion and Management*, 2007, **48**, 778-786.

[35] M.A.A. Mohammed, A. Salmiaton, W.A.K.G. Wan Azlina, M.S.M. Amran and A. Fakhru'l-Razi, *Energy Conversion and Management*, 2011, **52**, 1555-1561.

[36] J. Recari, C. Berrueco, S. Abelló, D. Montané and X. Farriol, *Fuel Processing Technology*, 2016, **142**, 107-114,.

[37] A.A. Khan, W. de Jong, P.J. Jansens and H. Spliethoff, *Fuel Processing Technology*, 2009, **90**, 21-50.

[38] H.K. Wyn, M. Konarova, J. Beltramini, G. Perkins and L. Yermán, *Fuel Processing Technology*, 2020, **205**, 106425.

[39] S.J. Yoon and J-G. Lee, *International Journal of Hydrogen Energy*, 2012, **37**, 17093-17100.

[40] A. Kumar, K. Eskridge, D.D. Jones and M.A. Hanna, *Bioresource Technology*, 2009, **100**, 2062-2068.

[41] Y. Song, Y. Tian, X. Zhou, S. Liang, X. Li, Y. Yang and L. Yuan, *Energy*, 2021, **226**, 2021, 120380.

[42] C. Sreejith, C. Muraleedharan and P. Arun. *International Journal of Ambient Energy, 2013, 34*, 35-52.

[43] X. Meng, W. De Jong, N. Fu and A.H.M. Verkooijen, *Biomass and Bioenergy*, 2011, **35**, 2910–2924.

[44] I. Narváez, A. Orío, M.P. Aznar and J. Corella, *Industrial & Engineering Chemistry Research,* 1996, **35,** 2110-2120.

[45] C. Lucas, D. Szewczyk, W. Blasiak and S. Mochida, *Biomass and Bioenergy*, 2004, **27**, 563-575.

[46] F. Yan, S-Y. Luo, Z-Q. Hu, B. Xiao and G. Cheng, *Bioresource Technology*, 2010, **101**, 5633-5637.

[47] L.E. Taba, M..F. Irfan, W.A.M.W. Daud and M.H. Chakrabarti, *Renewable and Sustainable Energy Reviews*, 2012, **16**, 5584-5596.

[48] M. Faraji and M. Saidi, *International journal of hydrogen energy, 2021,* **46**, 18844-18856.

[49] A. Gómez-Barea and B. Leckner, *Progress in Energy and Combustion Science*, 2010, **36**, 444-509.

[50] M. Puig-Arnavat, J.C. Bruno and A. Coronas, *Renewable and Sustainable Energy Reviews*, 2010, **14**, 2841-2851.

[51] S.L. Narnaware and N.L. Panwar, *Bioresource Technology Reports*, 2022, **17**, 100892.

[52] T.K. Patra and P.N. Sheth, *Renewable and Sustainable Energy Reviews*, 2015, **50**, 583-593.

[53] D.C. de Oliveira, E.E.S. Lora, O.J. Venturini, D.M.Y. Maya and M. Garcia-Pérez, *Renewable and Sustainable Energy Reviews*, 2023, **172**, 113047.

[54] X. Xiang, G. Gong, Y. Shi, Y. Cai and C. Wang, *Renewable and Sustainable Energy Reviews*, 2018, **82**, Part 3, 2768-2778.

[55] Q. He, Q. Guo, K. Umeki, Lu Ding, F. Wang and G. Yu, *Renewable and Sustainable Energy Reviews*, 2021, **139**, 110710.

[56] M. Costa, V. Rocco, C. Caputo, D. Cirillo, G. Di Blasio, M. La Villetta, G. Martoriello and R. Tuccillo, *Applied Thermal Engineering*, 2019, **160**, 114083.

[57] G.C. Umenweke, I.C. Afolabi, E.I. Epelle and J.A. Okolie, *Bioresource Technology Reports*, 2022, **17**, 100976.

[58] Y. Wu, H. Wang, H. Li, X. Han, M. Zhang, Y. Sun, X. Fan, R. Tu, Y. Zeng, C.C. Xu and X. Xu, *Renewable Energy*, 2022, **196**, 462-481.

[59] C. Li and K. Suzuki, *Renewable and Sustainable Energy Reviews*, 2009, **13**, 594-604.

[60] X. Zhang, A.C.K. Yip and S. Pang, *International Journal of Hydrogen Energy*, 2023, **48**, 10394-10422.

[61] A. Goel, E.M. Moghaddam, W. Liu, C. He and J. Konttinen, *Energy Conversion and Management*, 2022, **268**, 116020.

[62] D. Baruah and D.C. Baruah, *Renewable and Sustainable Energy Reviews*, 2014, **39**, 806-815.

[63] M. Mehrpooya, M. Khalili and M.M.M. Sharifzadeh, *Renewable and Sustainable Energy Reviews*, 2018, **91**, 869-887.

[64] M.L.Villetta, M. Costa and N. Massarotti, *Renewable and Sustainable Energy Reviews*, 2017, **74**, 71-88.

[65] H. Shahbeik, W. Peng, H. K. S. Panahi, M. Dehhaghi, G. J. Guillemin, A. Fallahi, H. Amiri, M. Rehan, D. Raikwar, H. Latine, B. Pandalone, B. Khoshnevisan, C. Sonne, L. Vaccaro, A.-S. Nizami, V. K. Gupta, S. S. Lam, J. Pan, R. Luque, B. Sels, M. Tabatabaei and M. Aghbashlo, *Renewable and Sustainable Energy Reviews*, 2022, **167**, 112833.

[66] S. Ascher, I. Watson and S. You, *Renewable and Sustainable Energy Reviews*, 2022, **155**, 111902, ISSN 1364-0321.

[67] J. Ren, J.-P. Cao, X.-Y. Zhao, F.-L. Yang and X.-Y. Wei. *Renewable and Sustainable Energy Reviews,* 2019, **116**, 109426.

[68] M. Ajorloo, M. Ghodrat, J. Scott and V. Strezov. *Journal of the Energy Institute*, 2022, **102**, 395-419.

[69] I.P. Silva, R.M.A. Lima, G.F. Silva, D.S. Ruzene and D.P. Silva, *Renewable and Sustainable Energy Reviews,* 2019, **114**, 109305.

[70] C.F. Palma. *Applied Energy*, 2013, **111**, 129-141

[71] A. Kushwah, T.R. Reina and M. Short, *Science of the Total Environment*, 2022, **834,** 155243.

[72] Y. Wang and C.M. Kinoshita. *Solar Energy*, 1993, **51**, 19-25.

[73] D.L. Giltrap, R. McKibbin and G.R.G. Barnes. *Solar Energy*, 2003, **74**, 85-91.

[74] M. B. Nikoo and N. Mahinpey. *Biomass and Bioenergy*, 2008, **32**, 1245-1254.

[75] M. Cortazar, G. Lopez, J. Alvarez, A. Arregi, M. Amutio, J. Bilbao and M. Olazar. *Chemical Engineering Journal*, **396**, 2020, 125200.

[76] B.V. Babu and P.N. Sheth. *Energy Conversion and Management*, 2006, **47**, 2602-2611.

[77] N. Gao and A. Li. *Energy Convers. Manag.*, 2008, **49,** 3483-3490.

[78] T.H. Jayah, L. Aye, R.J. Fuller, D.F. Stewart. *Biomass Bioenergy*, 2003, **25**, 459–469.

[79] A. Sharma. *Biomass and Bioenergy*, 2011, **35**, 4465–4473.

[80] Y. Gao and H. Li. *Bioresource Technology*, 2008. **99**, 3023–3033.

[81] G.H. Reman, *Chem. Ind.*, 1955, **3**, 46-51.

[82] R.C. Baliban, J.A. Elia and C.A. Floudas. *Comput. Chem. Eng.*, 2011, **35**, 1647-1690.

[83] Gómez-Barea and B. Leckner. *Prog. Energy Combust. Sci.*, 2010, **36**, 444-509.

[84] X. Li, J.R. Grace, A.P. Watkinson, C.J. Lim and A. Ergüdenler. *Fuel*, 2001, **80**, 195-207.

[84] K. Rabea, S. Michailos, M. Akram, K.J. Hughes, D. Ingham and M. Pourkashanian. *Energy Conversion and Management*, 2022, **258**. 115495.

[85] A. Gomez and N. Mahinpey. *Chemical engineering research and design*, 2005, **95**, 346-357.

[86] M. Barbanera, F. Cotana, and U.D. Matteo. *Renewable Energy,* 2018, **121**, 597-605.

[87] Q. Dang, X. Zhang, Y. Zhou and X. Jia(2021). *Fuel Processing Technology,* 2021, **212**, 106604.

[88] C.A. Koufopanos, A. Lucchesi and G. Maschio. Can. J. Chem. Eng, 1989, **67.**

[89] E. Shayan, V. Zare, and I. Mirzaee. *Energy Conversion and Management*, 2018, **159**, 30-41.

[90] A. Abuadala and I. Dincer. *Thermochimica Acta,* 2010, **507-508**, 127-134.

[91] R. Karamarkovic and V. Karamarkovic. *Energy,* 2010, **35,** 537-549.

[92] S. Sharma and P. Sheith (2016). *Energy Conversion Management*, 2016, **110**, 307-318.

[93] M. Hosseini, I. Dincer and M.A. Rosen. *International Journal of Hydrogen Energy,* 2012, **37**, 16446-16452.

[94] E. Balu, U. Lee and J. Chung. *International Journal of Hydrogen Energy,* 2015 **40**, 14104-14115.

[95] B.V. Babu and A.S. Chaurasia. *Energy Convers. Manag.*, 2003, **44**, 2135–2158.

[96] A. Melgar, J.F. Pérez, H. Laget and A. Horillo. *Energy Convers. Manag.,* 2007, **48**, 59–67.

[97] Z.A. Zainal, R. Ali, C.H. Lean and K.N. Seetharamu. *Energy Convers. Manag.*, 2001, **42**, 1499–1515.

[98] A. Mountouris, E. Voutsas and D.J.E.C. Tassios. *Energy Convers. Manag*., 2006, **47**, 1723–1737.

[99] M. Mehrpooya, M. Khalili and M. M. Sharifzadeh. *Renewable and Sustainable Energy Reviews,* 2018, **91**, 869-887.

[100] G. Schuster, G. Loffler, K. Weigl and H. Hofbauer. *Bioresource Technology,* 2001, **77**, 71-79.

[101] S. Vikram, P. Rosha, S. Kumar and S. Mahajani. (2022). *Energy,* 2022, **241**, 122854.

[102] T. Renganathan, M. Yadav, S. Pushpavanam, R. Voolapalli and Y. Cho. *Chemical Engineering Science,* 2012, **83**, 159-170.

[103] M. Mahishi and D. Goswami. *Internactional Journal of Hydrogen Energy,* 2007, **32**, 3831-3840.

[104] P. Chaiwatanodom, S. Vivanpatarakij and S. Assabumrungrat. *Applied Energy,* 2014, **114**, 10-17.

[105] S. Wang, X. Bi and S. *Energy,* 2015, **90**, 1207-1218.

[106] J. Kotowicz, A. Sobolewski and T. Iluk. *Energy,* 2013, **52**, 265-278.

[107] L. Abdelouahed O. Authier, G. Mauviel, J. P. Corriou, G. Verdier and A. Dufour. *Energy Fuels,* 2012, **26**, 3840-3855.

[108] M. Aneke and M. Wang. *Energy Procedia*, 2017, **142**, 829-834.

[109] M. Shamsi, A. A. Obaid, S. Farokhi and A. Bayat. *International Journal of Hydrogen Energy,* 2022, **47**, 772-781.

[110] T. Viertiö, V. Kivela, M. Putkonen, J. Kihlman and P. Simmel. *Catalysts,* 2021, **11**, 688.

[111] P. Weerachanchai, M. Horio, and C. Tangsathitkulchai. *Bioresource Technology,* 2009. 100, 1419-1427.

[112] S. Yang, M. Li, M. A. Nawaz, G. Song, W. Xiao, Z. Wang and D. Liu. *ACS omega,* 2020, **5**, 11701-11709.

[113] M.M. Khan, M.M., S. Xu, and C. Wang. *Journal of the Energy Institute,* 2021, **98**, 77-84.

[114] M. Yousefi, and S. Donne. *International Journal of Hydrogen Energy,* 2021, **47**, 699-727.

[115] S. Tanimura, H_2 Gas Turbine for Hydrogen Society EU-Japan Energy Business Seminar. https://www.eu-japan.eu/sites/default/files/imce/eu_jp_energy_business_seminar_mhps_r1.pdf.

[116] C.C. Chong, Y.W. Chen, K.H. Ng, D.V. N. Vo and M.K. Lam*. Fuel,* 2021, **311,** 122623.

[117] N. Gao, J. Salisu, C. Quan and P. Williams. *Renewable and Sustainable Energy Reviews,* 2021, **145**, 111023.

[118] G. Oh, S.Y. Park, M.W. Seo, Y.K. Kim, H.W. Ra, J.G. Lee and S.J. Yoon. *Renewable energy,* 2016, **86**, 841-847.

[119] Y. Pan, Y. Tursun, Y. Guo, H. Abduhani, A. Abulizi, D. Talifu and M. Zhong. Chemical Engineering & Technology, 2017, **45**, 1501-1511.

[120] G. Guan, M. Kaewpanha and X. Hao, A. Abudula. *Renewable and sustainable energy reviews,* 2016, **58**, 450-461.

[121] M.A. Gerber. *Review of novel catalysts for biomass tar cracking and methane reforming,* 2007, Pacific Northwest National Lab.(PNNL), Richland, WA (United States).

[122] R. Shakil, M.M.H. Rumon, Y.A. Tarek, C.K. Roy, A.N. Chowdhury and R. Das. *Surface-modified nanomaterials-based catalytic materials for water purification, hydrocarbon production, and pollutant remediation*. in: *Surface Modified Nanomaterials for Applications in Catalysis*. M. B. Gawande, C. M. Hussain, Y. Yamauchi, Elsevier, 2022,103-130. Boston, USA.

[123] Y. Chen, L. Guo, W. Cao, H, Jin, S. Guo and X. Zhang. *International Journal of Hydrogen Energy*, 2013, **38,** 12991-12999.

[124] Q. Ji, S. Tabassum, S. Hena, C.G. Silva, G. Yu and Z. Zhang. J*ournal of Cleaner Production*, 2016, **126**, 38-55.

[125] J. Ren, J.P. Cao, X. Y. Zhao, F.L. Yang and X.Y. Wei. *Renewable and Sustainable Energy Reviews,* 2019, **116**, 109426.

[126] M. Shahbaz, A. Inayat, D.O. Patrick and M. Ammar, Renew. Sustain. Energy Rev., 2017, 73, 468–476.

[127] Z. Zhang, L. Liu, B. Shen and C. Wu. *Renewable and Sustainable Energy Reviews,* 2018, **94**, 1086-1109.

[128] S.L. Narnaware, and N. Panwar. *Biomass Conversion and Biorefinery,* 2021, 1-31.

[129] M. Shahabuddin, Md. T. Alam, B. B. Krishna, T. Bhaskar and G. Perkins. *Bioresource Technology*, 2020, **312**, 123596.

[130] R. Zou, M. Qian, C. Wang, W. Mateo, Y. Wang, L. Dai, X. Lin, Y. Zhao, E. Huo, L. Wang, X. Zhang, X. Kong, R. Ruan and H. Lei. *Chemical Engineering Journal*, 2022, **441**, 135972.

[131] C. Berrueco, D. Montané, B. M. Güell and G. Del Alamo, Energy, 2014, 66, 849–859

[132] S. Hu, L. Jiang, Y. Wang, S. Su, L. Sun, B. Xu, L. He and J. Xiang, *Bioresour. Technol.*, 2015, **192**, 23–30.

[133] L. Jiang, S. Hu, Y. Wang, S. Su, L. Sun, B. Xu, L. He and J. Xiang, *Int. J. Hydrogen Energy*, 2015, **40**, 15460–15469.

[134] D. Sutton, B. Kelleher and J.R.H. Ross*, Fuel Process. Technol.,* 2001, **73**, 155–173.

[135] L. Dong, C. Wu, H. Ling, J. Shi, P.T. Williams and J. Huang, *Fuel*, 2017, **188**, 610–620.

[136] K. Murata, L. Wang, M. Saito, M. Inaba, I. Takahara and N. Mimura, *Energy & fuels*, 2004, **18**, 122–126.

[137] F.M. Alptekin and M. S. Celiktas, *ACS omega*, 2022, **7,** 24918–24941*.*

[138] J. De Greef, Q. N. Hoang, R. Vandevelde, W. Meynendonckx, Z. Bouchaar, G. Granata, M. Verbeke, M. Ishteva, T. Seljak and J. Van Caneghem, *Energies*, 2023, **16**, 1644.

[139] P. Aryal, A. Tanksale and A. Hoadley, *Int. J. Hydrogen Energy.,* 2023, **48**, 15014-15025.

[140] S. Das, K. H. Lim, T.Z. . Gani, S. Aksari and S. Kawi, *Appl. Catal. B Environ*., 2023, **323**, 122141.

[141] M. Fabrik, A. Salama and H. Ibrahim, *Fuel*, 2023, **347**, 128429*.*

[142] Z. Huang, Z. Deng, Y. Feng, T. Chen, D. Chen, A. Zheng, G. Wei, F. He, Z. Zhao and J. Wu, *ACS Sustain. Chem. Eng*., 2019, **7,** 16539–16548.

[143] S. Guo, X. Wei, D. Che, H. Liu and B. Sun. *Frontiers in Energy*, 2021, **15,** 374-383.

[144] I. Narvaez, A. Orio, M. P. Aznar and J. Corella. *Industrial & Engineering Chemistry Research*, 1996, **35**, 2110-2120.

[145] H. M. Yang, J. G. Liu, H. Zhang, X. X. Han and X. M. Jiang. *Energy Sources, Part A: Recovery, Utilization, and Environmental Effects,* 2019, **41**, 1993-2006.

[146] F. Benedikt, J. Fuchs, J. C. Schmid, S. Muller and H. Hofbauer. *Korean Journal of Chemical Engineering,* 2017, **34**, 2548-2558.

[147] J. C. Schmid, J. Fuchs, F. Benedik, A. M. Mauerhofer, S. Muller, H. Hofbauer, H. Stocher, N. Kieberger and T. Burgler. *Sorption enhanced reforming with the novel dual fluidized bed test plant at TU Wien*. in *European Biomass Conference and Exhibition (EUBCE). Stockholm*. 2017.

[148] J. Loipersböck, G. Weber, R. Rauch and H. Hofbauer. *Biomass Conversion and Biorefinery,* 2021, **11**, 85-94.

[149] Y. Tursun, S. Xu, A. Abulikemu and T. Dilinuer*. Bioresource technology,* 2019, **272**, 241-248.

[150] M. Asadullah, S-i. Ito, K. Kunimori and K. Tomishige. *Industrial & Engineering Chemistry Research,* 2002, **41**, 4567-4575.

[151] P. Lv, Z. Yuan, C. Wu, L. Ma, Y. Chen and N. Tsubaki. *Energy Conversion and Management,* 2007, **48**, 1132-1139.

[152] Y. Richardson, M. Drobek, A. Julbe, J. Blin and F. Pinta. *Biomass gasification to produce syngas*. in: *Recent advances in thermo-chemical conversion of biomass (Eds)*. A. Pandey, T. Bhaskar, M. Stocker, R.K. Sukumaran, Elsevier., 2015, 213-250. Boston, USA.

[153] J. Ren, Y.L. Liu, X.Y. Zhao and J.P. Cao. *Journal of the Energy Institute*, 2020, **93**, 1083-1098.

[154] X. Yang, S. Gu, A. Kheradmand and Y. Jiang. *Energy & Fuels,* 2021, **35**, 4997-5005.

[155] P. Šuhaj, J. Husár, and J. Haydary. *Sustainability,* 2020, **12**, 6647-6661.

[156] A. Kostyniuk, M. Grilc, and B. *Industrial & Engineering Chemistry Research,* 2019, **58**, 7690-7705.

[157] A. Soomro, S. Chen, S. Ma and W. Xiang. *Energy & Environment*, 2018, **29**, 839-867.

[158] J. Deng, K. Bu, Y. Shen, Z. Zhang, J. Zhang, K. Faungnawakij and D. Zhang. *Applied Catalysis B: Environmental,* 2022, **302**, 120859.

[159] Kattel, S., P. Atanassov, and B. Kiefer. *Physical Chemistry Chemical Physics,* 2013, **15**, 148-153.

[160] W. Li, H. Khalid, Z. Zhu, R. Zhang, G. Liu, C. Cheng and E. Thorin. *Applied Energy,* 2018, **226**, 1219-1228.

[161] N. Gautam and A. Chaurasia. *Journal of Material Cycles and Waste Management*, 2022, **24**, 166-178.

[162] S. Kumbhar and P.R. Bamane. *International Journal of Research Publication and Reviews*, **3**, 2392-2397.

[163] S. Shao, H. Zhang, R. Xiao, X. Li and Y. Cai. *Fuel Processing Technology,* 2018, **178**, 88-97.

[164] D. Wang, P. Jiang, H. Zhang and W. Yuan. *Science of the Total Environment,* 2020, **723**, 137775.

[165] Q. He, L. Ding, A. Raheem, Q. Guo, Y. Gong and G. Yu. *Chemical Engineering Journal,* 2021, **417**, 129331.

[166] X. Xiao, X. Meng, D. D. Le and T. Takarada. *Bioresource technology,* 2011, **102**, 1975-1981.

[167] D. Hu, X. Zeng, F. Wang, M.H. Adamu and G. Xu. *Fuel,* 2021, **290**, 120338.

[168] X. Zeng, F. Wang, Y. Wang, A. Li, J. Yu and G. Xu. *Energy & Fuels,* 2014, **29**, 1838-1845.

[169] X. Zeng, F. Wang, Z. Han, J. Han, J. Zhang, R. Wu and G. Xu. *Applied Energy,* 2019, **248**, 115-125.

[170] M. HarunaAdamu, X. Zeng*, J. Zhang, F. Wang and G. Xu. *International Journal of Hydrogen Energy,* 2022, **47**, 772-781.

[171] X. Zeng, Y. Ueki, R. Yoshiie, I. Naruse, F. Wang, Z. Han and G. Xu. *Fuel,* 2020, **264**, 116827.

[172] C. Wang, M. Zhang, Z. Han, D. Bai, W. Duo, X. Bi, A. Abudula, G. Guan and G. Xu. *Fuel,* 2021, **307**, 121816.

[173] X. Zeng, F. Wang, Z. Han, Y. Sun, Y. Cui and G. Xu. *Carbon Resources Conversion,* 2018, **1**, 73-80.

[174] M. Irfan, A. Li, L. Zhang, G. Li, Y. Gao and S. Khushk. *Waste Management,* 2021, **132**, 96-104.

[175] H.U. Modekwe, K. Moothi, M.O. Daramola and M.A. Mamo. *Polymers,* 2022, **14**, 2898.

[176] D. Buentello-Montoya, X. Zhang, S. Maques and M. Geron. *Energy Procedia,* 2019, **158**, 828-835.

[177] V. Benedetti, S. S. Ali, F. Patuzzi and M. Baratieri. *Frontiers in Chemistry,* 2019, **7**, 119.

[178] N. B. Klinghoffer, M.J. Castaldi, and A. Nzihou. *Fuel,* 2015, **157**, 37-47.

[179] Y. Zhang, Q. Shang, D. Feng, H. Sun, F. Wang, Z. Hu, Z, Cheng, Z. Zhou, Y. Zhao and S. Sun. *Fuel Processing Technology,* 2022, **233**, 107307.

[180] J. Meng, X. Wang, Z. Zhao, A. Zheng and Z. Huang. *Bioresource Technology,* 2018, **268**, 212-220.

[181] Courson, C. and K. Gallucci. *Gas cleaning for waste applications (syngas cleaning for catalytic synthetic natural gas synthesis)*. in: *Substitute natural gas from waste*. M. Materatzzi, P. U. Foscolo. Elsevier, 2019, 161-220. Boston, USA.

[182] E. Makó. *Journal of the European Ceramic Society,* 2007, **27,** 535-540.

[183] Z. Wang, P. Quyang, L. Cui, B. Zong, G. Wu and Y. Zhang. *Journal of the Energy Institute,* 2020, **93**, 2544-2549.

[184] S. C. Mojaki, S.B. Mishra, and A.K. Mishra. *ACS omega,* 2019, **4**, 20931-20936.

[185] J. Waluyo, P. M. Ruya, D. Hantoko, J. Rizkiana, I. G. B. N. Makerrtihartha, M. Yan and H. Susanto. *Bulletin of Chemical Reaction Engineering & Catalysis,* 2021, **16**, 623-631.

[186] S. Varjani. *Science of The Total Environment,* 2022, **836**, 155721.

[187] Y. Tian, X. Zhou, S. Lin, X. Ji, J. Bai and M. Xu. *Science of the Total Environment,* 2018, **645**, 518-523.

[188] M. Thakkar, J. P. Makwana, P. Mohanty, M. Shah and V. Singh. *Industrial Crops and Products*, 2016, **87**, 324-332.

[189] F. Miccio, B. Piriou, G. Ruoppolo and R. Chirone. *Chemical Engineering Journal,* 2009, **154**, 369-374.

[190] S. Rapagnà, N. Jand, A. Kiennemann and P.U. Foscolo. *Biomass and bioenergy,* 2000, **19**, 187-197.

[191] M. Niu, Y. Huang, B. Jin and Y. Sun. *Chemical Engineering & Technology*, 2014, **37**, 1787-1796.

[192] C. Zhou, C. Rosén, and K. Engvall. *Fuel Processing Technology,* 2017, **159**, 460-473.

[193] T. Pröll, R. Rauch and C. Aichernig. *International Journal of Chemical Reactor Engineering,* 2007, **5**, doi.org/10.2202/1542-6580.1398

[194] M. Cortazar, S. Sun, C. Wu, L. Santamaria, L. Olazar, E. Fernandez, M. Artetxe, G. Lopez and M. Olazar, J. Environ. Chem. Eng., 2021, **9**, 106725.

[195] H. Abduhani, Y. Tursun, M. Zhong and X. Huang. *Fuel,* 2022. **322**, 124100.

[196] B.A. Oni, S.E. Sanni and S.O. Oyedepo. *Journal of the Energy Institute,* 2022, **103**, 33-46.

[197] H. Li, Y. Wang, N. Zhou, L. Dai, W. Deng, C. Liu. Y. Cheng, Y. Liu, K, Chobb, P. Chen and R. Ruan. *Journal of Cleaner Production,* 2021, **291**, 125826.

[198] B. Li, H. Yang, L. Wei, J. Shao, X. Wang and H. Chen. *International Journal of Hydrogen Energy,* 2017, **42**, 4832-4839.

[199] B. Acharya, A. Dutta, and P. Basu. *International Journal of Hydrogen Energy,* 2010, **35**, 1582-1589.

[200] L. Han, Q. Wang, Y. Yang, C. Yu, M. Fang and Z. Luo. *International journal of hydrogen energy,* 2011, **36**, 4820-4829.

[201] B. Acharya, A. Dutta, and P. Basu. *Energy & Fuels,* 2009, **23**, 5077-5083.

[202] H. Guoxin, and H. Hao. *Biomass and Bioenergy,* 2009, **33**, 899-906.

[203] M. Shahbaz, A. Inayat, D.O. Patrik and M. Ammar. *Renewable and Sustainable Energy Reviews,* 2017, **73**, 468-476.

[204] K. Mitsuoka, S. Hayashi, H. Amano, K. Kayahara, E. Sasaoaka and M.D.A. Uddin. *Fuel Processing Technology,* 2011, **92**, 26-31.

[205] P. Lv, J. Chang, T. Wang, Y. Fu, Y. Chen and J. Zhu. *Energy & Fuels,* 2004, **18**, 228-233.

[206] E. Tezel, E.B. Unlu, H.E. Figen and S.Z. Baykara. *International Journal of Hydrogen Energy,* 2020, **45**, 34739-34748.

[207] M.P. Orihuela, P. Miceli, J. Ramirez-Rico, D. Fino and R. Chacategui. *Chemical Engineering Journal,* 2021, **415**, 128959.

[208] D. Dayton, *Review of the literature on catalytic biomass tar destruction: Milestone completion report.* 2002.

[209] M. Lim, and Z. Alimuddin. *Reduction of tar from biomass gasification using a dielectric barrier discharge reactor.* in: *IOP Conference Series: Materials Science and Engineering.* 2021. IOP Publishing.

[210] A. S. Al-Rahbi, and P.T. Williams. *Waste Disposal & Sustainable Energy,* 2022, **4**, 75-89.

[211] B. Zhao, X. Zhang, L. Chen, R. Qu, G. Meng, X. Yi and L. Sun. *Biomass and Bioenergy,* 2010, **34**, 140-144.

[212] H.J. Park, S.H. Park, J.M. Sohn, I. Park, J-K. Jeon, S-S. Kim and Y-K Park. *Bioresource technology,* 2010, **101**, S101-S103.

[213] A. Jess. *Fuel,* 1996, **75**, 1441-1448.

[214] S.R. de la Rama, S. Kawai, H. Yamada, and T. Tagawa. *Journal of Catalysts,* 2013, **2013**, 1-7.

[215] A. Paethanom, S. Nakahara, M. Kobayashi, P. Prawisudha and K. Yoshikawa. *Fuel processing technology,* 2012, **104**, 144-154.

[216] I. Sharma, A.F.A. Hoadley, S. M. Mahajani and A. Ganesh, *Journal of Cleaner Production*, 2016, **119**, 196-206.

[217] P. Aravind, and W. de Jong. *Progress in Energy and Combustion Science,* 2012, **38**, 737-764.

[218] M. C. dos Santos, T.M. Basegio, L. A.C. Tarelho and C.P. Bergmann. *Nanostructured Catalysts for Biomass Gasification*. In: Kopp Alves, A. (eds) Environmental Applications of Nanomaterials. Engineering Materials. Springer, 2021, 97-107. https://doi.org/10.1007/978-3-030-86822-2_6.

[219] I. Shimada, C. Uno, Y. Watanabe and T. Takatsuka. *Fuel Processing Technology,* 2022, **232,** 107267.

[220] M.D. Argyle and C.H. Bartholomew. *Catalysts,* 2015, **5**, 145-269.

[221] P.R. Buchireddy, D. Peck, M. Zappi and R.M. Bricka. *Energies,* 2021, **14**, 1875.

[222] J.I. Villacampa, C. Royo, E. Romeo, J.A. Montoya, P. Del Angel and A. Monzón. *Applied Catalysis A: General,* 2003, **252**, 363-383.

[223] J. Kotowicz, A. Sobolewski, and T. Iluk. *Energy,* 2013, **52**, 265-278.

[224] M. Parvez and M. *Biofuels,* 2015, **6**, 369-373.

[225] S. Islam and I. Dincer, I. *Journal of Energy Resources Technology Transactions,* 2018, **140**, 9.

[226] N. Asgari, R. K. Saray and S. Mirmasoumi. *Energy Conversion and Management,* 2020, **220**, 113096.

[227] M. Aneke, and M. Wang. *Energy Procedia,* 2017, **142**, 829-834.

[228] C. Wang, H. Jin, P. Peng and J. Chen. *Renewable Energy,* 2019, **141,** 1117-1126.

[229] N. T. Ngoc Lan Thao, K.-Y. Chiang, H.-P. Wan, W.-C. Hung and C.-F. Liu, *International Journal of Hydrogen Energy*, 2019, **44**, 3363-3372.

[230] K. M. Broer, P. J. Woolcock, P. A. Johnston and R. C. Brown, *Fuel*, 2015, **140**, 282-292.

[231] A. Riaz, G. Zahedi and J.J. Klemeš, *Journal of Cleaner Production*, 2013, **57**, 19-37.

[232] R. Rauch, J. Hrbek and H. Hofbauer, *Wiley Interdisciplinary Reviews: Energy and Environment*, 2014, **3**, 343-362.

[233] N. Koizumi, K. Murai, T. Ozaki and M. Yamada, *Catalysis Today*, 2004, **89**, 465-478.

[234] H. Boerrigter, H.P. Calis and D.J. Slort, *ECN Report ECN-C–04-056*, 2004.

[235] Y. Zhang and H. Ahn, *Energy*, 2019, **173**, 1273-1284.

[236] M. Ramdin, A. Amplianitis, S. Bazhenov, A. Volkov, V. Volkov, T.J.H. Vlugt and T.W. de Loos, *Industrial & Engineering Chemistry Research*, 2014, **53**, 15427-15435.

[237] A. Masudi, N.W.C. Jusoh and O. Muraza, *Catalysis Science & Technology*, 2020, **10**, 1582-1596.

[238] X. Xue, Y. Weng, S. Yang, S. Meng, Q. Sun and Y. Zhang, *RSC Advances*, 2021, **11**, 6163-6172.

[239] V. Subramani and S.K. Gangwal, *Energy & Fuels*, 2008, **22**, 814-839.

[240] X. Xiaoding, E.B.M. Doesburg and J.J.F. Scholten, *Catalysis Today*, 1987, **2**, 125-170.

[241] W.U. Khan, L. Baharudin, J. Choi and A.C.K. Yip, *ChemCatChem*, 2020, **13**, 111-120.

[242] K. Xiao, Z. Bao, X. Qi, X. Wang, L. Zhong, M. Lin, K. Fang and Y. Sun, *Catalysis Communications*, 2013, **40**, 154-157.

[243] D. Liuzzi, F.J. Pérez-Alonso and S. Rojas, *Fuel*, 2021, **293**.

[244] H.M. Koo, T. Tran-Phu, G.-R. Yi, C.-H. Shin, C.-H. Chung and J.-W. Bae, *Catalysis Science & Technology*, 2016, **6**, 4221-4231.

[245] B. Hou, X.-Y. Han, M.-G. Lin and K.-G. Fang, *Journal of Fuel Chemistry and Technology*, 2016, **44**, 217-224.

[246] Y. Fang, Y. Liu, W. Deng and J. Liu, *Journal of Energy Chemistry*, 2014, **23**, 527-534.

[247] H. Zhang, W. Chu, H. Xu and J. Zhou, *Fuel*, 2010, **89**, 3127-3131.

[248] Y. Li, W. Gao, M. Peng, J. Zhang, J. Sun, Y. Xu, S. Hong, X. Liu, X. Liu, M. Wei, B. Zhang and D. Ma, *Nat Commun*, 2020, **11**, 61.

[249] J. Xia, D. Mao, B. Zhang, Q. Chen, Y. Zhang and Y. Tang, *Catalysis Communications*, 2006, **7**, 362-366.

[250] T. Takeguchi, K.-i. Yanagisawa, T. Inui and M. Inoue, *Applied Catalysis A: General*, 2000, **192**, 201-209.

[251] H.S. Jung, F. Zafar, X. Wang, T.X. Nguyen, C.H. Hong, Y.G. Hur, J.W. Choung, M.-J. Park and J.W. Bae, *ACS Catalysis*, 2021, **11**, 14210-14223.

[252] R. Phienluphon, K. Pinkaew, G. Yang, J. Li, Q. Wei, Y. Yoneyama, T. Vitidsant and N. Tsubaki, *Chemical Engineering Journal*, 2015, **270**, 605-611.

[253] M. Gentzen, D.E. Doronkin, T.L. Sheppard, A. Zimina, H. Li, J. Jelic, F. Studt, J. D. Grunwaldt, J. Sauer and S. Behrens, *Angew Chem Int Ed Engl*, 2019, **58**, 15655-15659.

[254] J.-S. Jung, G. Hong, E.-H. Yang, Y. S. Noh and D. J. Moon, *Journal of Nanoscience and Nanotechnology*, 2016, **16**, 10397-10403.

[255] G.H. Hong, Y.S. Noh, J.I. Park, S.A. Shin and D.J. Moon, *Catalysis Today*, 2018, **303**, 136-142.

[256] H.M. Koo, C.-I. Ahn, D.H. Lee, H.-S. Roh, C.-H. Shin, H. Kye and J.W. Bae, *Fuel*, 2018, **225**, 460-471.

[257] D. Liuzzi, F. Pérez-Alonso and S. Rojas, *Fuel*, 2021, **293**, 120435.

[258] H. Liu, R. Zhang, L. Ling, Q. Wang, B. Wang and D. Li, *Catalysis Science & Technology*, 2017, **7**, 3758-3776.

[259] Y. Qi, J. Yang, D. Chen and A. Holmen, *Catalysis Letters*, 2014, **145**, 145-161.

[260] L. Zhao, J. Zhu, Y. Zheng, M. Xiao, R. Gao, Z. Zhang, G. Wen, H. Dou, Y. P. Deng, A. Yu, Z. Wang and Z. Chen, *Advanced Energy Materials*, 2021, **12**.

[261] J. Greeley, I. E. Stephens, A. S. Bondarenko, T. P. Johansson, H. A. Hansen, T. F. Jaramillo, J. Rossmeisl, I. Chorkendorff and J. K. Norskov, *Nat Chem*, 2009, **1**, 552-556.

[262] T. Murakami, H. Wakabayashi, D. Maruoka and E. Kasai, *ISIJ International*, 2020, **60**, 2678-2685.

[263] K. Nishioka, Y. Ujisawa, S. Tonomura, N. Ishiwata and P. Sikstrom, *Journal of Sustainable Metallurgy*, 2016, **2**, 200-208.

[264] J. Liang, N. Li, Z. Zhao, L. Ma, X. Wang, S. Li, X. Liu, T. Wang, Y. Du, G. Lu, J. Han, Y. Huang, D. Su and Q. Li, *Angew Chem Int Ed Engl*, 2019, **58**, 15471-15477.

[265] S. Sharma and B. G. Pollet, *Journal of Power Sources*, 2012, **208**, 96-119.

[266] Z. Qiao, S. Hwang, X. Li, C. Wang, W. Samarakoon, S. Karakalos, D. Li, M. Chen, Y. He, M. Wang, Z. Liu, G. Wang, H. Zhou, Z. Feng, D. Su, J. S. Spendelow and G. Wu, *Energy & Environmental Science*, 2019, **12**, 2830-2841.

[267] K.L.M. Gang Wu, Christina M. Johnston and Piotr Zelenay, *Science*, 2010, **332**, 443-337.

[268] P. Xu, X. Han, C. Wang, B. Zhang, X. Wang and H.-L. Wang, *Macromolecular Rapid Communications*, 2008, **29**, 1392-1397.

[269] S.-Y. Huang, P. Ganesan, S. Park and B. N. Popov, *Journal of the American Chemical Society*, 2009, **131**, 13898-13899.

[270] K. Sasaki, L. Zhang and R.R. Adzic, *Phys Chem Chem Phys*, 2008, **10**, 159-167.

[271] C. Xu, C. Fan, X. Zhang, H. Chen, X. Liu, Z. Fu, R. Wang, T. Hong and J. Cheng, *ACS Appl Mater Interfaces*, 2020, **12**, 19539-19546.